Biochemical and Biophysical Research Communications 395 (2010) 565–571

Contents lists available at ScienceDirect

Biochemical and Biophysical Research Communications

journal homepage: www.elsevier.com/locate/ybbrc

Biological properties of purified recombinant HCV particles with an epitope-tagged envelope

Hitoshi Takahashi [a,b], Daisuke Akazawa [a,b], Takanobu Kato [a], Tomoko Date [a], Masayuki Shirakura [a,b], Noriko Nakamura [b], Hidenori Mochizuki [b], Keiko Tanaka-Kaneko [c], Tetsutaro Sata [c], Yasuhito Tanaka [d], Masashi Mizokami [e], Tetsuro Suzuki [a], Takaji Wakita [a,*]

[a] Department of Virology II, National Institute of Infectious Diseases, Tokyo, Japan
[b] Toray Industries, Inc., Kanagawa, Japan
[c] Department of Pathology, National Institute of Infectious Diseases, Tokyo, Japan
[d] Department of Clinical Molecular Informative Medicine, Nagoya City University Graduate School of Medicine, Nagoya, Japan
[e] Research Center for Hepatitis & Immunology, Kohnodai Hospital, International Medical Center of Japan, Chiba, Japan

ARTICLE INFO

Article history:
Received 3 April 2010
Available online 23 April 2010

Keywords:
Hepatitis C virus
Envelope protein
Purification
Particle
Vaccine

ABSTRACT

To establish a simple system for purification of recombinant infectious hepatitis C virus (HCV) particles, we designed a chimeric J6/JFH-1 virus with a FLAG (FL)-epitope-tagged sequence at the N-terminal region of the E2 hypervariable region-1 (HVR1) gene (J6/JFH-1/1FL). We found that introduction of an adaptive mutation at the potential *N*-glycosylation site (E2N151K) leads to efficient production of the chimeric virus. This finding suggests the involvement of glycosylation at Asn within the envelope protein(s) in HCV morphogenesis.

To further analyze the biological properties of the purified recombinant HCV particles, we developed a strategy for large-scale production and purification of recombinant J6/JFH-1/1FL/E2N151K. Infectious particles were purified from the culture medium of J6/JFH-1/1FL/E2N151K-infected Huh-7 cells using anti-FLAG affinity chromatography in combination with ultrafiltration. Electron microscopy of the purified particles using negative staining showed spherical particle structures with a diameter of 40–60 nm and spike-like projections. Purified HCV particle-immunization induced both an anti-E2 and an anti-FLAG antibody response in immunized mice. This strategy may contribute to future detailed analysis of HCV particle structure and to HCV vaccine development.

1. Introduction

The hepatitis C virus (HCV) causes chronic hepatitis, liver cirrhosis and hepatocellular carcinoma [1]. HCV is a positive strand RNA virus belonging to the *Hepacivirus* genus in the Flaviviridae family. The HCV genome consists of about 9600 nucleotides and contains three regions: a 5′ non-coding region of 341 nucleotides containing the sequence for the IRES structure, a coding region of about 9000 nucleotides, which encodes about 10 viral proteins, and a 3′ non-coding region of about 200 nucleotides depending on the size of the poly-uridylate track within this region [2,3].

The main therapy for HCV is treatment with pegylated-interferon and rivabirin. However, these agents show little effect in patients that have a high titer of HCV RNA, genotype 1. Thus, it is necessary to develop new, more effective therapies and preventive treatments to counteract HCV infection. As yet, no preventive vaccine is available for HCV. A recombinant HCV vaccine based on the viral envelope protein E1/E2 has been reported that generated neutralizing antibodies (nAb) in animals [4]. These nAbs were capable of limiting HCV pseudoparticles (HCVpp) and HCV cell culture (HCVcc) infection.

Recently, a genotype 2a strain of HCV named JFH-1 was discovered. This strain can efficiently replicate in the Huh-7 cell line [5], and an *in vitro* culture system of infectious HCV has also been successfully developed using the JFH-1 genome [6–8]. The JFH-1 viral production system is expected to become a powerful tool for HCV vaccine development. In this study, we developed a simple strategy for purification of recombinant HCV particles from the media of infected Huh-7 cells for structural analysis and for vaccine development using the JFH-1 genome.

2. Materials and methods

2.1. Plasmids

Plasmid pJ6/JFH-1 was generated from pJFH-1 by replacement of the 5′ untranslated region with the p7 region of J6 [9]. The

* Corresponding author. Address: Department of Virology II, National Institute of Infectious Diseases, 1-23-1 Toyama, Shinjuku, Tokyo 162-8640, Japan. Fax: +81 3 5285 1161.
E-mail address: wakita@nih.go.jp (T. Wakita).

0006-291X/$ - see front matter © 2010 Elsevier Inc. All rights reserved.
doi:10.1016/j.bbrc.2010.04.081

plasmids pJ6/JFH-1/1FL and pJ6/JFH-1/3FL were constructed by introduction of a single (DYKDDDDKGGG) or triple (DYKDHDG-DYKDHDIDYKDDDDKGGG) FLAG-tag sequence, respectively, into pJ6/JFH-1, which replaced part of the E2 HVR1 (amino acids 394–400) region. These two plasmids were then modified by introduction of a Lys residue to replace the Asn at amino acid position 151 of the E2 sequence, creating pJ6/JFH-1/1FL/E2N151K and pJ6/JFH-1/3FL/E2N151K, respectively.

The J6E2 gene (codons 1490–2500) was generated by PCR amplification from pJ6CF. The sense and antisense primers used were: 5′-CACAAGCTTCGCACCCATACTGTTGGGG-3′ and 5′-ACAGGATCCCAT-CGGACGATGTATTTTGTG-3′, respectively. For cloning purposes, HindIII or BamHI sites (underlined) were added to the primers. The amplified DNA was digested and inserted into p3XFLAG-CMV-13 (SIGMA, Saint Louis, MO).

The plasmid CDM-J6E2Fc encodes the J6E2 sequence downstream of the preprotrypsin leader sequence. pCDM-J6E2Fc was digested with SacI and BamHI, and the DNA fragment containing the preprotrypsin leader and J6E2 sequence was inserted into pCD4Rg (a kind gift from Dr. Brian Seed, Harvard Medical School) from which the SacI–BamHI fragment containing the CD4 gene was removed. This ligation resulted in the creation of a plasmid encoding a fusion gene of E2 and human IgG1-Fc.

2.2. Cell culture

The human hepatoma cell line, Huh-7, was maintained in DMEM supplemented with 10% FBS at 37 °C in a 5% CO_2 incubator.

2.3. In vitro synthesis of HCV RNA and RNA transfection of Huh cells

HCV RNA was synthesized from the plasmids described above *in vitro* using a MEGAscript T7 kit (Ambion, Austin, TX). Synthesized HCV RNA was then electroporated into cells as previously described [10]. The transfected cells were transferred onto 100-mm culture dishes containing culture medium.

2.4. Quantification of HCV core protein and RNA

The HCV core protein in cell culture supernatants or in purified HCV samples was quantified by enzyme immunoassay using a HCV core ELISA kit (Ortho Clinical Diagnostics). HCV RNA in purified HCV samples was quantified by RTD-PCR as previously described [11].

2.5. Deglycosylation with PNGase F

For deglycosylation reactions, the Enzymatic In-Solution N-Deglycosylation kit (Sigma) was used according to the manufacturer's instructions. Briefly, lysates of passaged cells were incubated for 10 min at 100 °C in denaturation buffer and then in the presence of PNGase F enzyme for 1 h at 37 °C. These samples were analyzed by Western blotting as described below using anti-FLAG (SIGMA) and anti-GAPDH (CHEMICON, Temecula, CA) antibodies.

2.6. Sequence analysis

The cDNAs of the HCV genome were synthesized from total RNA isolated from HCV RNA-transfected cells [5]. These cDNA were subsequently amplified using DNA polymerase (*TaKaRa LA Taq*, Takara, Shiga, Japan). The sequence of the amplified DNA was determined by the 3130 Genetic Analyzer (Applied Biosystems, Foster city, CA).

2.7. Purification of recombinant HCV particles

Culture supernatants from Huh-7 cells transfected with FLAG-tagged HCV RNA were harvested. The medium was concentrated by ultrafiltration using the pellicon-2 300 system (Millipore, Bedford, MA) and was subjected to affinity chromatography using an Anti-FLAG M2 affinity gel (Sigma). Virus particles were eluted using the 3×FLAG Peptide (Sigma) and were concentrated by ultracentrifugation for 2 h at 50,000 rpm at 4 °C.

2.8. Determination of the viral infectious titer

The infectious titer was determined by the method as previously described and was expressed as the number of focus-forming units per milliliter (FFU/mL) [6].

2.9. Western blotting

The purified HCV sample was lysed using a buffer containing 0.1 M Tris–HCl (pH 6.8), 4% SDS, 1.2% 2-mercaptoethanol, 20% glycerol, and Bromophenol blue. SDS–PAGE and immunoblotting were performed as previously described [6]. Antibodies used for immunoblotting were: anti-HCV core (clone 2H9) [6], anti-E1 (B7567) [6], and anti-E2 (clone 8D10-3, unpublished).

2.10. Electron microscopy

Concentrated, purified HCV particles were allowed to settle on carbon-coated copper grids and were stained with 4% uranylacetate. The grids were examined in a transmission electron microscope (H-7650, Hitachi, Tokyo, Japan) and were photographed at an instrumental magnification of 50,000×.

2.11. Sucrose density gradient analysis

The purified HCV sample containing 266 fmol of the HCV core was layered on a stepwise sucrose gradient (10–60%, wt/vol) and was centrifuged for 16 h in an SW41 rotor (Beckman Coulter, Fullerton, CA) at 35,000 rpm at 4 °C. After centrifugation, 12 fractions were harvested from the bottoms of the tubes. For each fraction, the core protein concentration was determined using an immunoassay. The HCV RNA titer was determined using RTD-PCR. The infectious titer was determined using an immunofluorescence assay as described above.

2.12. HCV particle-immunization

The purified HCV particles described above were inactivated by UV-irradiation, and 2 pmol of the HCV core protein of the particles were intraperitoneally injected into 4 week old BALB/c female mice ($n = 3$). Immunization was repeated four times at 2-week intervals (0, 2, 4 and 6 weeks). The Sigma Adjuvant System (Sigma), composed of monophosphoryl lipid A and trehalose dicorynomycolate, was used as an adjuvant. Saline alone was injected into control mice. Sera were collected at 1, 3, 5 and 7 weeks after immunization.

2.13. EIA for measurement of anti-E2 and anti-FLAG antibody responses

Recombinant J6E2/Fc or the FLAG peptide antigen (Sigma) was bound to microtiter plates (Nunc, Rochester, NY, USA) overnight at 4 °C, at a concentration of 50 ng per well. Recombinant J6E2/Fc was produced from COS-1 cells transfected with the CDM-J6E2Fc plasmid, which encodes the J6CF-E2 region (aa 384–720) fused with the Fc region of human IgG. The plates were blocked with Blocking One solution (Nacalai Tesque, Kyoto, Japan) and were washed with PBS containing 0.05% Tween 20 (washing buffer). Serum samples were diluted in washing buffer and were transferred to the blocked, antigen coated plates. After a 1.5-h incubation,

the plates were washed and bound antibody was detected using an HRP-conjugated anti-mouse antibody (GE healthcare, Buckinghamshire, England) and 3,3′,5,5′-tetramethylbenzidine (TMBZ) as a substrate (Sumitomo Bakelite, Tokyo, Japan).

3. Results

3.1. Production of recombinant HCV with an epitope-tagged envelope

To facilitate purification of recombinant HCV particles secreted into the culture medium of transfected cells, we constructed recombinant HCV with a FLAG-epitope-tagged envelope, which could then be purified by affinity chromatography using an anti-FLAG-agarose column. The FLAG-tagged HCV genome J6/JFH-1/3FL with the J6CF structural region was constructed by introducing a triple FLAG-tag sequence into the HVR1 of E2 (Fig. 1A). This region was selected for epitope-tag insertion because we predicted that this region would lie on the outside of the virus particles and would be tolerant to amino acid changes. Recombinant HCV particles were produced following transfection of Huh-7 cells with viral RNA, and were secreted into the culture medium.

RNA-transfected cells were passaged every 4 or 5 days. The level of the HCV core protein in the culture supernatant was measured over a period of 70 days (Fig. 1B). In contrast to the gradually increasing level of the core protein in J6/JFH-1 cells over time, the level of the core protein in the supernatants of the J6/JFH-1/3FL RNA-transfected cells decreased over the first 3 weeks post-transfection. Subsequently, the level began to increase and this level became equal to that of the wild-type J6/JFH-1 RNA-transfected cells 35 days post-transfection. This result suggested that after the first 35 days of culture, some mutations were introduced into the HCV genome that conferred efficient virus production during genome replication and/or that the transfected cells were altered in some way that was more favorable for viral production.

3.2. An N151K mutation facilitates the production of FLAG-tagged HCV

To determine if any adaptive mutations had arisen in the viral genome, we sequenced the full length of the HCV genome on days 8 and 35 post-J6/JFH-1/3FL RNA transfection. On day 8 post-transfection, no non-synonymous mutations were detected. However, on day 35, we found a single amino acid mutation at a potential

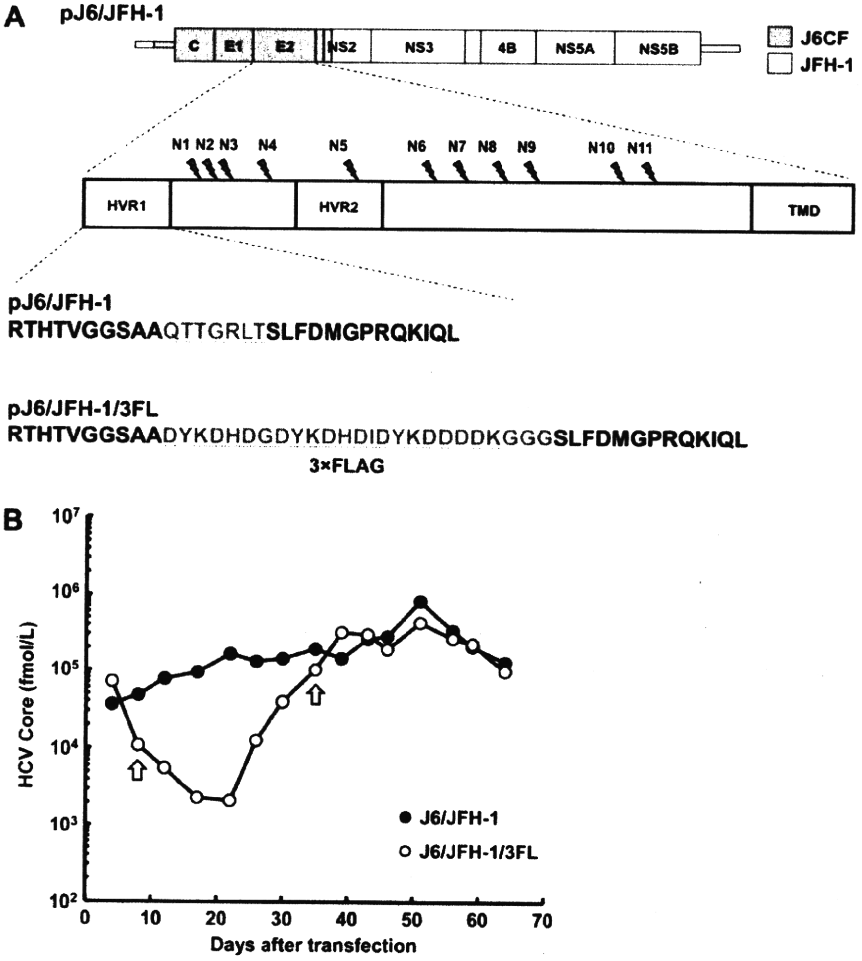

Fig. 1. Time course of HCV core protein secretion in recombinant HCV RNA-transfected cells. (A) Organization of the recombinant HCV construct pJ6/JFH-1/3FL. Open reading frames (thick boxes) are flanked by 5′- and 3′-UTRs (thin boxes). Gray, J6CF; white, JFH-1; HVR, hyper variable region; TMD, transmembrane domain. *N*-Glycosylation sites are indicated by pointers and are numbered N1–N11. The region of pJ6/JFH-1 that is replaced by the 3×FLAG sequence to generate pJ6/JFH-1/3FL is indicated at bottom. (B) HCV core protein secretion into the culture medium after HCV RNA transfection of Huh-7 cells. The HCV core protein was analyzed using an ELISA. Arrows indicate the times at which the J6/JFH-1/3FL HCV genome transfected into HCV RNA-transfected cells was sequenced.

N-glycosylation site of the E2 protein (Fig. 2A) in which asparagine at amino acid position 151 in the E2 protein was changed to lysine (E2N151K). Interestingly, this mutation was identical to that described by Delgrange et al. [12] as a mutation that was important for efficient production of HCV JFH-1. We performed Western blot analysis of cell lysates of transfected cells of different passages, using the anti-FLAG antibody as a probe for E2, to confirm that the N151K mutation abolishes one specific *N*-glycosylation. Indeed, the size of the FLAG-E2 protein was smaller on days 30 and 43 compared to that on day 4 (Fig. 2B). In contrast, the size of FLAG-E2 proteins that were deglycosylated using PNGase F was similar for all of the tested samples (Fig. 2B). This result suggested that the E2N151K mutation abolished *N*-glycosylation at this residue.

To investigate if the E2N151K mutation enhances production of FLAG-tagged HCV, we introduced the E2N151K mutation into the J6/JFH-1/3FL genome (J6/JFH-1/3FL/E2N151K). J6/JFH-1/3FL/E2N151K RNA-transfected cells were then passaged every 4 or 5 days and the level of the HCV core protein in the culture supernatant was measured over a period of 16 days (Fig. 2C). The result clearly showed that the E2N151K mutation contributes to efficient production of FLAG-tagged HCV particles.

We further analyzed the effect of the E2N151K mutation on specific viral infectivity (Table 1). The culture supernatant on day 3 post-transfection of recombinant viral RNA was therefore concentrated by ultrafiltration and tested in an infectious assay. The recombinant virus with the E2N151K mutation exhibited higher specific infectivity than the virus without this mutation. These data suggest that efficient production of infectious particles is impaired by the introduction of a FLAG-tag into the E2 protein but that this deficiency could be compensated for by the introduction of the E2N151K mutation which modifies an *N*-glycosylation site.

3.3. Purification of FLAG-tagged HCV

To purify FLAG-tagged HCV particles, we used a viral construct with a single FLAG-tag, J6/JFH-1/1FL/E2N151K (Fig. 1A), which as efficient in virus production as J6/JFH-1/3FL/E2N151K (data not shown). A total of 10 L of the culture supernatant of Huh-7 cells infected with J6/JFH-1/1FL/E2N151K was collected. This culture medium was concentrated to 300 mL by ultrafiltration and was then subjected to affinity chromatography using an anti-FLAG-agarose column. Bound virus particles were eluted using 10 mL of a

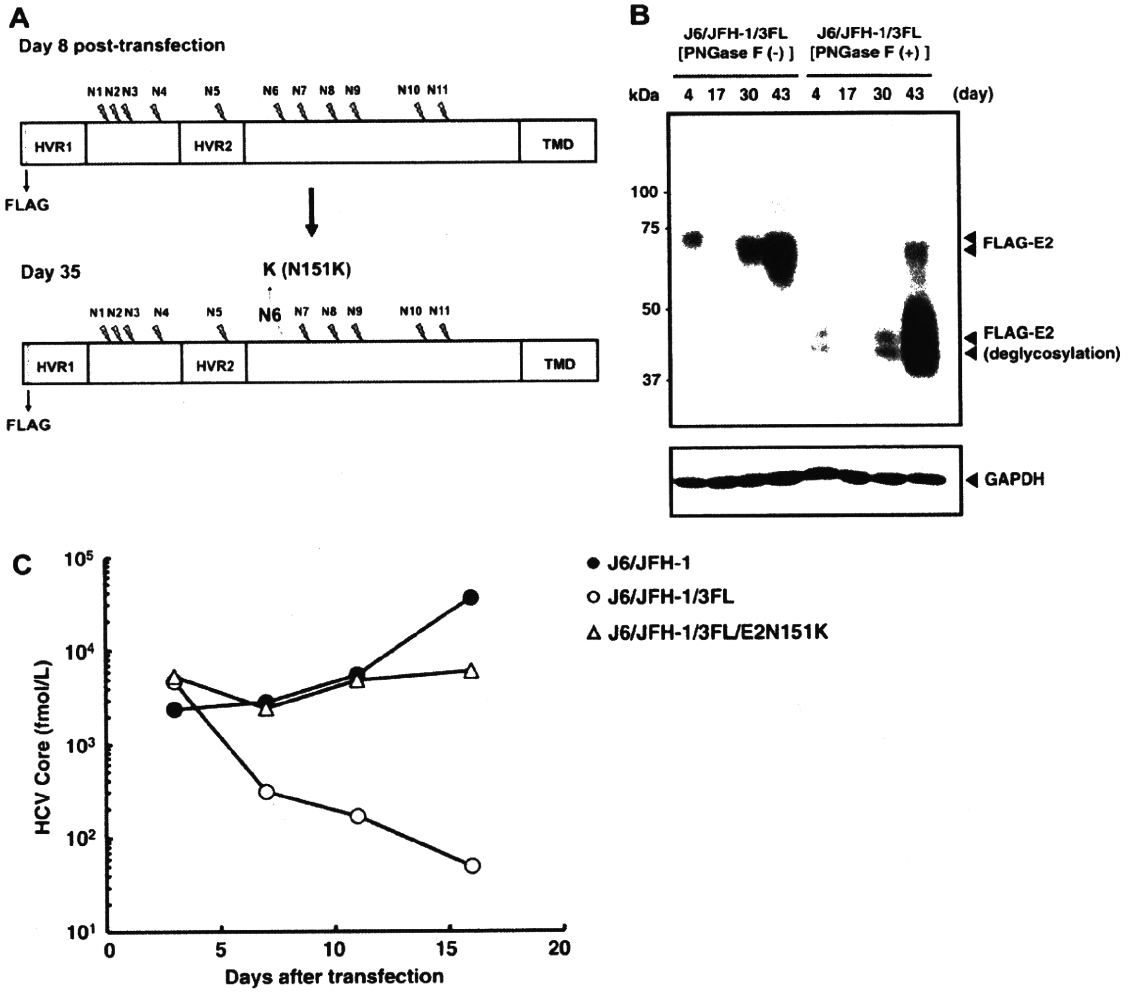

Fig. 2. Characterization of the recombinant HCV genome with an introduced N151K mutation. (A) Schematic diagram of the sequence of the E2 in the J6/JFH-1/3FL HCV RNA-transfected cells on day 8 and day 35 post-transfection. N151K replaces an Asn residue with a Lys residue at the N6 glycosylation site of E2. (B) Western blot analysis of the FLAG-E2 protein in lysates of cells transfected with J6/JFH-1/3FL RNA. Arrowheads indicate intact, and deglycosylated (PNGase F (+)), FLAG-E2 protein (upper panel) and control GAPDH protein (lower panel). (C) HCV core protein secretion into the culture medium following transfection of Huh-7 cells with HCV RNA with or without an introduced N151K mutation.

Table 1
Infectivity of recombinant viruses with or without N151K mutation.

Recombinant virus	Infectious titer ($\times 10^2$ FFU/mL)	HCV core protein ($\times 10^2$ fmol/mL)	Specific infectivity (FFU/HCV core)
J6/JFH-1/3FL	<1.7	1.6	<1.1
J6/JFH-1/3FL/E2N151K	8.3	2.0	4.2

FLAG peptide solution. Finally, the purified HCV particles were concentrated by ultracentrifugation.

The HCV yield and the amount of total protein after each purification step are summarized in Table 2. This purification process resulted in a 5000-fold concentration of the culture supernatant. The recovery of the HCV core protein in the final purified virus preparation was approximately 5%, and the virus purity was increased about 9000-fold compared to its purity in the initial culture medium. Specific infectivity was increased about 4-fold after the final step.

HCV structural proteins in the purified virus sample were examined by Western blotting (Fig. 3A). Core, E1 and E2 proteins were all detected in the purified virus preparation. Interestingly, incorporation of the E2 protein into the purified virus appeared to increase compared to incorporation of the core and E1 proteins. However, this higher apparent incorporation of FLAG-E2, may reflect the presence of free, non-virus incorporated FLAG-E2 proteins that co-purified with the FLAG-tagged virus. We further analyzed the virus particles in the purified preparation by electron microscopy (Fig. 3B–D). Substantial debris was found in the culture

Table 2
HCV yield and properties of purified recombinant HCV after each purification step.

Purification step	Volume (mL)	HCV core protein ($\times 10^2$ fmol/mL)	HCV RNA ($\times 10^7$ copies/mL)	Total protein (μg/mL)	Recovery[a] (%)	Purity[b]	Infectivity ($\times 10^2$ FFU/mL)	Specific infectivity (FFU/HCV core)
Culture supernatant	10,000	1.4	3.5	877	100	1	25	18
Concentrate (after Ultrafiltration)	300	45	57	19,597	96	0.73	743	17
Affinity purification (after Elution)	10	98	324	171	7	469	4240	43
Concentrate (after Ultracentrifugation)	0.2	1440	3220	84	5	9546	94,600	66

[a] Recovery of HCV core protein.
[b] The degree of virus purity was calculated by HCV RNA contents per μg total proteins.

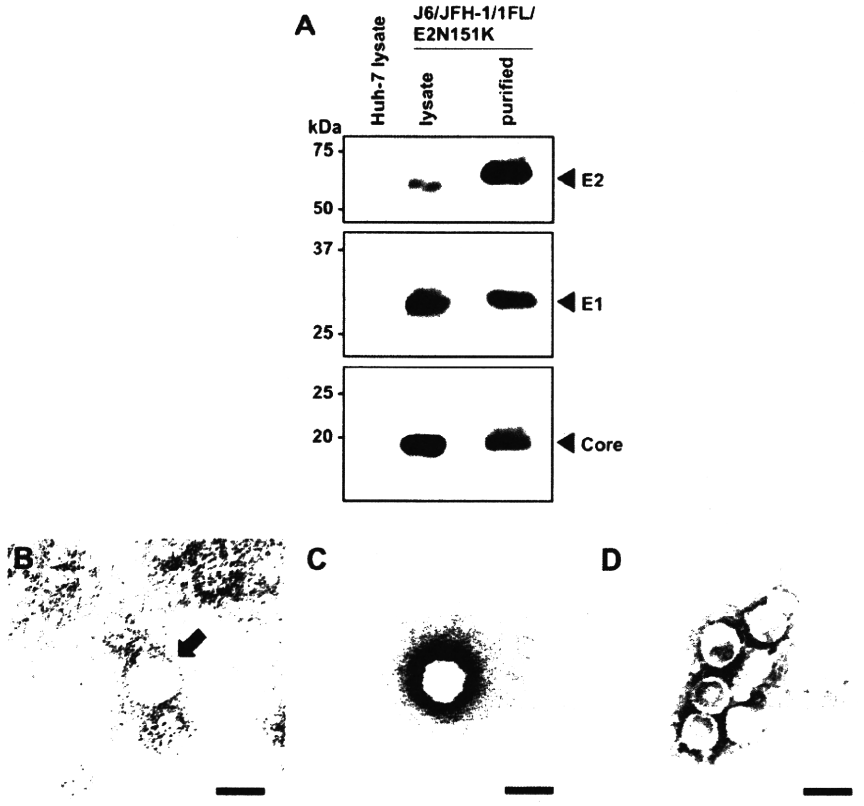

Fig. 3. Analysis of purified HCV particles. (A) Western blot analysis of viral proteins in lysates of, and in HCV particles purified from, whole-cell extracts of Huh-7 cells transfected with J6/JFH-1/1FL N151K RNA. Lysates of non-transfected cells were also analyzed. The arrowheads indicate the positions of the HCV core, E1 and E2 proteins. Marker proteins are shown at left. (B–D) Electron micrographs using negative staining of: (B) An HCV particle from culture media (indicated by an arrow.), (C) A purified HCV particle and (D) Purified HCV particles aggregated by an anti-FLAG antibody. Scale bar, 50 nm.

supernatant concentrated by ultrafiltration, which made it difficult to identify virus particles (Fig. 3B). In contrast, spherical particle structures of 40–60 nm could be clearly observed in the purified samples (Fig. 3C and D). Furthermore, the purified FLAG-tagged HCV particles were aggregated by the anti-FLAG antibody (Fig. 3D). The size and morphology of the FLAG-tagged particles were similar to each other but with slight deviations. The combined data suggest that the FLAG-tagged HCV particles can be purified by affinity chromatography using anti-FLAG-agarose.

3.4. Physical properties of purified FLAG-tagged HCV

We next further analyzed the properties of the purified FLAG-tagged HCV particles. The total number of proteins in the purified viral sample, as judged by SDS–PAGE and silver staining analysis, was much lower than that in the original culture medium (Fig. 4A). We confirmed by mass spectrometry analysis that these extra protein bands in the purified preparation were not viral proteins but were host proteins that bound to the FLAG-agarose (data not shown).

We further analyzed the purified FLAG-tagged HCV particles using a sucrose density gradient (Fig 4B). Purified virus was layered on top of a preformed continuous 10–60% sucrose gradient and was then centrifuged. Twelve fractions were collected and the HCV core protein, RNA and viral infectivity were determined for each fraction. The HCV particles migrated at a density between 1.13 and 1.16 g sucrose/mL. The density at which the peak of the HCV core protein was observed was almost identical to the density at which the HCV RNA and infectivity were detected.

3.5. Immunogenicity of purified HCV particles

To examine the immunogenicity of the FLAG-tagged HCV particles, they were injected into BALB/c mice and the sera of these mice were then analyzed for reactivity with recombinant J6E2/Fc or the FLAG peptide using an ELISA. The HCV particles were inactivated by UV-irradiation prior to injection using the Sigma Adjuvant System as an adjuvant. Both anti-E2 and anti-FLAG antibodies were induced in mice sera after four immunizations (Fig. 4C). These results suggested that the envelope proteins of the FLAG-tagged HCV

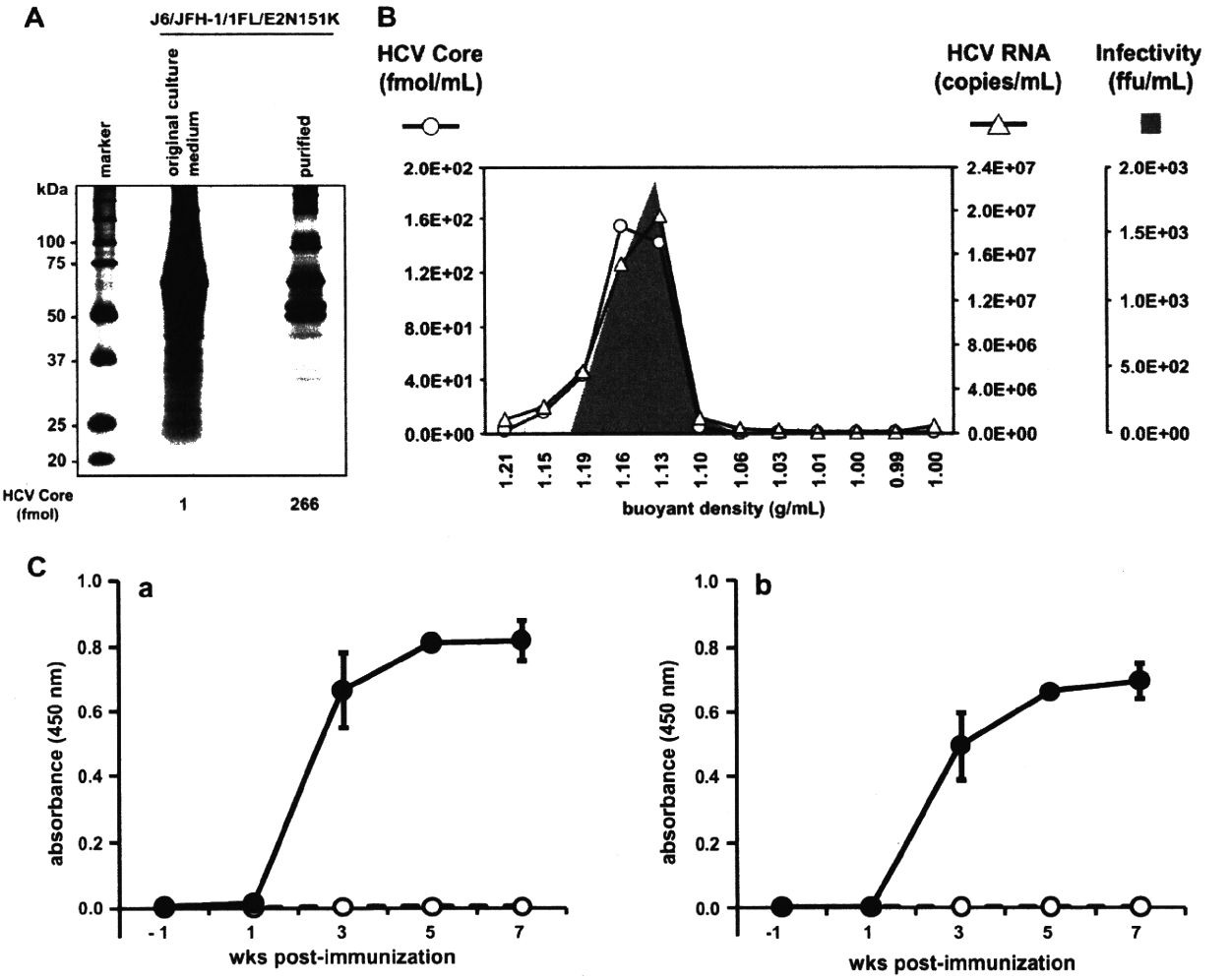

Fig. 4. Physical properties and immunogenicity of purified HCV particles. (A) Silver staining of non-purified (original culture medium) and purified HCV samples. The non-purified and purified samples contained 1 and 266 fmol, respectively, of the HCV core. (B) Sucrose density gradient analysis of purified HCV particles. The level of the HCV core protein (open circles), HCV RNA (open triangles) and the HCV infectivity towards naïve Huh-7 cells (shown in gray) were analyzed for each fraction as described in Section 2. (C) Purified HCV particles (closed circles) or saline (open circles) were intraperitoneally injected into BALB/c mice ($n = 3$), and sera were collected at the indicated times. The collected sera were examined for the presence of anti-E2 (a) and anti-FLAG (b) antibodies using the J6E2/Fc protein and the FLAG peptide as antigens in an EIA as described in Section 2.

particles were immunogenic and that insertion of a tag into the E2 protein could induce antibodies as a secondary immunogen.

4. Discussion

In this study we showed that infectious FLAG-tagged HCV particles with an N151K mutation that modulated HCV-glycosylation could be efficiently produced in cells and purified on a FLAG-agarose column. This purification procedure allowed analysis of the physical properties of the particles and the generation of anti-E2 antibodies.

The FLAG-tagged HCV particles were purified by simple anti-FLAG affinity chromatography in combination with ultrafiltration. However, the efficiency of purification was low, and the recovery of the HCV core protein in the final purified virus preparation was only approximately 5%. This low efficiency of purification of the HCV particles maybe due to a number of factors: (1) Interaction between the E2-FLAG protein and the anti-FLAG-agarose column may have been prevented by cellular host proteins with specific or non-specific affinity for the anti-FLAG-agarose, (2) A conformation change may have occurred in the E2 protein due to insertion of the FLAG sequence, which may have blocked FLAG interaction with anti-FLAG, (3) Free FLAG-E2 proteins may have bound more tightly to the FLAG-agarose than the FLAG-E2 protein on the viral surface. Nevertheless, sufficient purified FLAG-HCV particles were obtained with this purification procedure for further analysis.

In the density gradient analysis of the purified HCV particles, the peak of the HCV core protein coincided with the peaks of HCV RNA and viral infectivity. In previous reports of density gradient fractionation of non-FLAG-tagged viral particles, the peak of infectivity was reported to shift to a lighter density fraction than the peaks of HCV core protein or RNA [8,13,14]. This discrepancy between our, and previous, data may be explained by the fact that the properties of the purified FLAG-tagged HCV particles may differ from those of the JFH-1 based HCV particles reported previously. Regarding viral infectivity, it is known that cholesterol and sphingolipid association with HCV particles is important for virion maturation and infectivity [9]. The association of HCV particles with these lipids occurs in lipid rafts [9]. Since the E2-FLAG protein may have a decreased dependency on lipid rafts compared to the non-tagged E2 protein, this therefore resulted in a shift in the peak of infectivity. Alternatively, an association between HCV and very-low-density lipoprotein (VLDL) has an important role in HCV infectivity [15]. Tagging of HCV particles with FLAG may have somehow changed the association of HCV with VLDL and cause the observed shift in the infectivity peak. The mechanism of the shift of the infectivity peak of the FLAG-HCV particles needs to be examined in more detail in future studies.

HCV particles from human plasma samples have been previously examined by immunogold electron microscopy [16]. In the present study, we could clearly observe spherical particle structures of 40–60 nm in the purified samples. Furthermore, the FLAG-tagged HCV particles were aggregated by anti-FLAG antibody. This is the first report of the aggregation of HCV particles produced in an *in vitro* culture system. This method may therefore facilitate future examination of the detailed conformation of HCV particles and future elucidation of HCV particle structure by cryo-electron microscopy. However, it is regarded structural analysis as difficult to that aggregated HCV particles were inequable showing in this report because of this method also gathered defective viral particles which have the E2-FLAG protein.

Immunization of mice with purified FLAG-tagged HCV particles induced anti-E2 as well as anti-FLAG antibodies. These results indicated that the envelope proteins of the FLAG-tagged HCV particles were immunogenic and that insertion of a tag into the E2 protein could induce antibodies as a secondary immunogen. Thus, not only epitopes of viral origin, but also an epitope inserted into the virus, can induce an immune response. Although it is unclear how many amino acids can be inserted into the E2 HVR1, at least a triple FLAG-tag sequence (25 amino acids) is possible as shown in this study.

In conclusion, we have established a simple system for the purification of recombinant infectious FLAG-epitope-tagged HCV particles. The use of this system may contribute to studies aimed at a detailed analysis of HCV particle structure and towards HCV vaccine development.

Acknowledgments

This work was partially supported by a grant-in-aid for Scientific Research from the Japan Society for the Promotion of Science, from the Ministry of Health, Labor and Welfare of Japan, by the Research on Health Sciences Focusing on Drug Innovation from the Japan Health Sciences Foundation, and by the Japanese Society of Gastroenterology.

References

[1] K. Shimotohno, Hepatitis C virus as a causative agent of hepatocellular carcinoma, Intervirology 38 (1995) 162–169.
[2] Q.L. Choo, K.H. Richman, J.H. Han, K. Berger, C. Lee, C. Dong, C. Gallegos, D. Coit, R. Medina-Selby, P.J. Barr, A.J. Weiner, D.W. Bradley, G. Kuo, M. Houghton, Genetic organization and diversity of the hepatitis C virus, Proc. Natl. Acad. Sci. USA 88 (1991) 2451–2455.
[3] N. Kato, M. Hijikata, Y. Ootsuyama, M. Nakagawa, S. Ohkoshi, T. Sugimura, K. Shimotohno, Molecular cloning of the human hepatitis C virus genome from Japanese patients with non-A, non-B hepatitis, Proc. Natl. Acad. Sci. USA 87 (1990) 9524–9528.
[4] Z. Stamataki, S. Coates, M.J. Evans, M. Wininger, K. Crawford, C. Dong, Y.L. Fong, D. Chien, S. Abrignani, P. Balfe, C.M. Rice, J.A. McKeating, M. Houghton, Hepatitis C virus envelope glycoprotein immunization of rodents elicits cross-reactive neutralizing antibodies, Vaccine 25 (2007) 7773–7784.
[5] T. Kato, T. Date, M. Miyamoto, A. Furusaka, K. Tokushige, M. Mizokami, T. Wakita, Efficient replication of the genotype 2a hepatitis C virus subgenomic replicon, Gastroenterology 125 (2003) 1808–1817.
[6] T. Wakita, T. Pietschmann, T. Kato, T. Date, M. Miyamoto, Z. Zhao, K. Murthy, A. Habermann, H.G. Krausslich, M. Mizokami, R. Bartenschlager, T.J. Liang, Production of infectious hepatitis C virus in tissue culture from a cloned viral genome, Nat. Med. 11 (2005) 791–796.
[7] J. Zhong, P. Gastaminza, G. Cheng, S. Kapadia, T. Kato, D.R. Burton, S.F. Wieland, S.L. Uprichard, T. Wakita, F.V. Chisari, Robust hepatitis C virus infection in vitro, Proc. Natl. Acad. Sci. USA 102 (2005) 9294–9299.
[8] B.D. Lindenbach, M.J. Evans, A.J. Syder, B. Wolk, T.L. Tellinghuisen, C.C. Liu, T. Maruyama, R.O. Hynes, D.R. Burton, J.A. McKeating, C.M. Rice, Complete replication of hepatitis C virus in cell culture, Science 309 (2005) 623–626.
[9] H. Aizaki, K. Morikawa, M. Fukasawa, H. Hara, Y. Inoue, H. Tani, K. Saito, M. Nishijima, K. Hanada, Y. Matsuura, M.M. Lai, T. Miyamura, T. Wakita, T. Suzuki, Critical role of virion-associated cholesterol and sphingolipid in hepatitis C virus infection, J. Virol. 82 (2008) 5715–5724.
[10] M.J. van den Hoff, A.F. Moorman, W.H. Lamers, Electroporation in 'intracellular' buffer increases cell survival, Nucleic Acids Res. 20 (1992) 2902.
[11] T. Takeuchi, A. Katsume, T. Tanaka, A. Abe, K. Inoue, K. Tsukiyama-Kohara, R. Kawaguchi, S. Tanaka, M. Kohara, Real-time detection system for quantification of hepatitis C virus genome, Gastroenterology 116 (1999) 636–642.
[12] D. Delgrange, A. Pillez, S. Castelain, L. Cocquerel, Y. Rouille, J. Dubuisson, T. Wakita, G. Duverlie, C. Wychowski, Robust production of infectious viral particles in Huh-7 cells by introducing mutations in hepatitis C virus structural proteins, J. Gen. Virol. 88 (2007) 2495–2503.
[13] D. Akazawa, T. Date, K. Morikawa, A. Murayama, N. Omi, H. Takahashi, N. Nakamura, K. Ishii, T. Suzuki, M. Mizokami, H. Mochizuki, T. Wakita, Characterization of infectious hepatitis C virus from liver-derived cell lines, Biochem. Biophys. Res. Commun. 377 (2008) 747–751.
[14] Y. Miyanari, K. Atsuzawa, N. Usuda, K. Watashi, T. Hishiki, M. Zayas, R. Bartenschlager, T. Wakita, M. Hijikata, K. Shimotohno, The lipid droplet is an important organelle for hepatitis C virus production, Nat. Cell Biol. 9 (2007) 1089–1097.
[15] S.U. Nielsen, M.F. Bassendine, A.D. Burt, C. Martin, W. Pumeechockchai, G.L. Toms, Association between hepatitis C virus and very-low-density lipoprotein (VLDL)/LDL analyzed in iodixanol density gradients, J. Virol. 80 (2006) 2418–2428.
[16] M. Kaito, S. Watanabe, H. Tanaka, N. Fujita, M. Konishi, M. Iwasa, Y. Kobayashi, E.C. Gabazza, Y. Adachi, K. Tsukiyama-Kohara, M. Kohara, Morphological identification of hepatitis C virus E1 and E2 envelope glycoproteins on the virion surface using immunogold electron microscopy, Int. J. Mol. Med. 18 (2006) 673–678.

JOURNAL OF VIROLOGY, June 2010, p. 5824–5835 Vol. 84, No. 11
0022-538X/10/$12.00 doi:10.1128/JVI.02397-09

Production of Infectious Hepatitis C Virus by Using RNA Polymerase I-Mediated Transcription▽

Takahiro Masaki,[1]† Ryosuke Suzuki,[1]† Mohsan Saeed,[1,4] Ken-ichi Mori,[2] Mami Matsuda,[1] Hideki Aizaki,[1] Koji Ishii,[1] Noboru Maki,[2] Tatsuo Miyamura,[1] Yoshiharu Matsuura,[3] Takaji Wakita,[1] and Tetsuro Suzuki[1]*

Department of Virology II, National Institute of Infectious Diseases, Shinjuku-ku, Tokyo 162-8640, Japan[1]; Advanced Life Science Institute, Wako, Saitama 351-0112, Japan[2]; Department of Molecular Virology, Research Institute for Microbial Diseases, Osaka University, Suita-shi, Osaka 565-0871, Japan[3]; and Graduate School of Medicine, The University of Tokyo, Tokyo 113-0033, Japan[4]

Received 13 November 2009/Accepted 8 March 2010

In this study, we used an RNA polymerase I (Pol I) transcription system for development of a reverse genetics protocol to produce hepatitis C virus (HCV), which is an uncapped positive-strand RNA virus. Transfection with a plasmid harboring HCV JFH-1 full-length cDNA flanked by a Pol I promoter and Pol I terminator yielded an unspliced RNA with no additional sequences at either end, resulting in efficient RNA replication within the cytoplasm and subsequent production of infectious virions. Using this technology, we developed a simple replicon *trans*-packaging system, in which transient transfection of two plasmids enables examination of viral genome replication and virion assembly as two separate steps. In addition, we established a stable cell line that constitutively produces HCV with a low mutation frequency of the viral genome. The effects of inhibitors of N-linked glycosylation on HCV production were evaluated using this cell line, and the results suggest that certain step(s), such as virion assembly, intracellular trafficking, and secretion, are potentially up- and downregulated according to modifications of HCV envelope protein glycans. This Pol I-based HCV expression system will be beneficial for a high-throughput antiviral screening and vaccine discovery programs.

Over 170 million people worldwide have been infected with hepatitis C virus (HCV) (22, 33, 37), and persistence of HCV infection is one of the leading causes of liver diseases, such as chronic hepatitis, cirrhosis, and hepatocellular carcinoma (16, 25, 38). The HCV genome is an uncapped 9.6-kb positive-strand RNA sequence consisting of a 5′ untranslated region (UTR), an open reading frame encoding at least 10 viral proteins (Core, E1, E2, p7, NS2, NS3, NS4A, NS4B, NS5A, and NS5B), and a 3′UTR (46). The structural proteins (Core, E1, and E2) reside in the N-terminal region.

The best available treatment for HCV infection, which is pegylated alpha interferon (IFN-α) combined with ribavirin, is effective in only about half of patients and is often difficult to tolerate (25). To date, a prophylactic or therapeutic vaccine is not available. There is an urgent need to develop more effective and better tolerated therapies for HCV infection. Recently, a robust system for HCV production and infection in cultured cells has been developed. The discovery that some HCV isolates can replicate in cell cultures and release infectious particles has allowed the complete viral life cycle to be studied (23, 49, 53). The most robust system for HCV production involves transfection of Huh-7 cells with genomic HCV RNA of the JFH-1 strain by electroporation. However, using this RNA transfection system, the amount of secreted infectious viruses often fluctuate and mutations emerge in HCV genome with multiple passages for an extended period of time (54), which limits its usefulness for antiviral screening and vaccine development.

DNA-based expression systems for HCV replication and virion production have also been examined (5, 15, 21). With DNA-based expression systems, transcriptional expression of functional full-length HCV RNA is controlled by an RNA polymerase II (Pol II) promoter and a self-cleaving ribozyme(s). DNA expression systems using RNA polymerase I (Pol I) have been utilized in reverse genetics approaches to replicate negative-strand RNA viruses, including influenza virus (12, 29), Uukuniemi virus (11), Crimean-Congo hemorrhagic fever virus (10), and Ebola virus (13). Pol I is a cellular enzyme that is abundantly expressed in growing cells and transcribes rRNA lacking both a 5′ cap and a 3′ poly(A) tail. Thus, viral RNA synthesized in cells transfected with Pol I-driven plasmids containing viral genomic cDNA has no additional sequences at the 5′- or 3′ end even in the absence of a ribozyme sequence (28). The advantages of DNA-based expression systems are that DNA expression plasmids are easier to manipulate and generate stable cell lines that constitutively express the viral genome.

We developed here a new HCV expression system based on transfection of an expression plasmid containing a JFH-1 cDNA clone flanked by Pol I promoter and terminator sequences to generate infectious HCV particles from transfected cells. The technology presented here has strong potential to be the basis for *trans*-encapsidation system by transient transfection of two plasmids and for the establishment of an efficient and reliable screening system for potential antivirals.

MATERIALS AND METHODS

DNA construction. To generate HCV-expressing plasmids containing full-length JFH1 cDNA embedded between Pol I promoter and terminator se-

* Corresponding author. Present address: Department of Infectious Diseases, Hamamatsu University School of Medicine, Hamamatsu 431-3192, Japan. Phone: 81-53-435-2336. Fax: 81-53-435-2337. E-mail: tesuzuki@hama-med.ac.jp.

† T.M. and R.S. contributed equally to this study.

▽ Published ahead of print on 17 March 2010.

quences, part of the 5′UTR region and part of the NS5B to the 3′UTR region of full-length JFH-1 cDNA were amplified by PCR using primers containing BsmBI sites. Each amplification product was then cloned into a pGEM-T Easy vector (Promega, Madison, WI) and verified by DNA sequencing. Both fragments were excised by digestion with NotI and BsmBI, after which they were cloned into the BsmBI site of the pHH21 vector (a gift from Yoshihiro Kawaoka, School of Veterinary Medicine, University of Wisconsin-Madison [29]), which contains a human Pol I promoter and a mouse Pol I terminator. The resultant plasmid was digested by AgeI and EcoRV and ligated to JFH-1 cDNA digested by AgeI and EcoRV to produce pHHJFH1. pHHJFH1/GND having a point mutation at the GDD motif in NS5B to abolish RNA-dependent RNA polymerase activity and pHHJFH1/R783A/R785A carrying double Arg-to-Ala substitutions in the cytoplasmic loop of p7 were constructed by oligonucleotide-directed mutagenesis. To generate pHHJFH1/ΔE carrying in-frame deletions of parts of the E1 and E2 regions (amino acids [aa] 256 to 567), pHHJFH1 was digested with NcoI and AscI, followed by Klenow enzyme treatment and self-ligation. To generate pHH/SGR-Luc carrying the bicistronic subgenomic HCV reporter replicon and its replication-defective mutant, pHH/SGR-Luc/GND, AgeI-SpeI fragments of pHHJFH1 and pHHJFH1/GND were replaced with an AgeI-SpeI fragment of pSGR-JFH1/Luc (20). In order to construct pCAG/C-NS2 and pCAG/C-p7, PCR-amplified cDNA for C-NS2 and C-p7 regions of the JFH-1 strain were inserted into the EcoRI sites of pCAGGS (30). In order to construct stable cell lines, a DNA fragment containing a Zeocin resistance gene excised from pSV2/Zeo2 (Invitrogen, Carlsbad, CA) was inserted into pHH21 (pHHZeo). Full-length JFH-1 cDNA was then inserted into the BsmBI sites of pHHZeo. The resultant construct was designated pHHJFH1/Zeo.

Cells and compounds. The human hepatoma cell line, Huh-7, and its derivative cell line, Huh7.5.1 (a gift from Francis V. Chisari, The Scripps Research Institute), were maintained in Dulbecco modified Eagle medium (DMEM) supplemented with nonessential amino acids, 100 U of penicillin/ml, 100 μg of streptomycin/ml, and 10% fetal bovine serum (FBS) at 37°C in a 5% CO_2 incubator. *N*-Nonyl-deoxynojirimycin (*N*N-DNJ) and kifunensine (KIF) were purchased from Toronto Research Chemicals (Ontario, Canada), castanospermine (CST) and 1,4-dideoxy-1,4-imino-D-mannitol hydrochloride (DIM) were from Sigma-Aldrich (St. Louis, MO), 1-deoxymannojirimycin (DMJ) and swainsonine (SWN) were from Alexis Corp. (Lausen, Switzerland), and *N*-butyl-deoxynojirimycin (*N*B-DNJ) was purchased from Wako Chemicals (Osaka, Japan). BILN 2061 was a gift from Boehringer Ingelheim (Canada), Ltd. These compounds were dissolved in dimethyl sulfoxide and used for the experiments. IFN-α was purchased from Dainippon-Sumitomo (Osaka, Japan).

DNA transfection and selection of stable cell lines. DNA transfection was performed by using FuGENE 6 transfection reagent (Roche, Mannheim, German) in accordance with the manufacturer's instructions. To establish stable cell lines constitutively producing HCV particles, pHHJFH1/Zeo was transfected into Huh7.5.1 cells within 35-mm dishes. At 24 h posttransfection (p.t.), the cells were then divided into 100-mm dishes at various cell densities and incubated with DMEM containing 0.4 mg of zeocin/ml for approximately 3 weeks. Selected cell colonies were picked up and amplified. The expression of HCV proteins was confirmed by measuring secreted core proteins. The stable cell line established was designated H751JFH1/Zeo.

***In vitro* synthesis of HCV RNA and RNA transfection.** RNA synthesis and transfection were performed as previously described (26, 49).

RNA preparation, Northern blotting, and RNase protection assay (RPA). Total cellular RNA was extracted with a TRIzol reagent (Invitrogen), and HCV RNA was isolated from filtered culture supernatant by using the QIAamp viral RNA minikit (Qiagen, Valencia, CA). Extracted cellular RNA was treated with DNase (TURBO DNase; Ambion, Austin, TX) and cleaned up by using an RNeasy minikit, which includes another step of RNase-free DNase digestion (Qiagen). The cellular RNA (4 μg) was separated on 1% agarose gels containing formaldehyde and transferred to a positively charged nylon membrane (GE Healthcare, Piscataway, NJ). After drying and cross-linking by UV irradiation, hybridization was performed with [α-^{32}P]dCTP-labeled DNA using Rapid-Hyb buffer (GE Healthcare). The DNA probe was synthesized from full-length JFH-1 cDNA using the Megaprime DNA labeling system (GE Healthcare). Quantification of positive- and negative-strand HCV RNA was performed using the RPA with biotin-16-uridine-5′-triphosphate (UTP)-labeled HCV-specific RNA probes, which contain 265 nucleotides (nt) complementary to the positive-strand (+) 5′UTR and 248 nt complementary to the negative-strand (−) 3′UTR. Human β-actin RNA probes labeled with biotin-16-UTP were used as a control to normalize the amount of total RNA in each sample. The RPA was carried out using an RPA III kit (Ambion) according to the manufacturer's procedures. Briefly, 15 μg of total cellular RNA was used for hybridization with 0.3 ng of the β-actin probe and 0.6 ng of either the HCV (+) 5′UTR or (−) 3′UTR RNA probe. After digestion with RNase A/T1, the RNA products were analyzed by electrophoresis in a 6% polyacrylamide–8 M urea gel and visualized by using a chemiluminescent nucleic acid detection module (Thermo Scientific, Rockford, IL) according to the manufacturer's instructions.

Reverse transcriptase PCR (RT-PCR), sequencing, and rapid amplification of cDNA ends (RACE). Aliquots (5 μl) of RNA solution extracted from filtered culture supernatant were subjected to reverse transcription with random hexamer and Superscript II reverse transcriptase (Invitrogen). Four fragments of HCV cDNA (nt 129 to 2367, nt 2285 to 4665, nt 4574 to 7002, and nt 6949 to 9634), which covers most of the HCV genome, were amplified by nested PCR. Portions (1 or 2 μl) of each cDNA sample were subjected to PCR with TaKaRa LA *Taq* polymerase (Takara, Shiga, Japan). The PCR conditions consisted of an initial denaturation at 95°C for 2 min, followed by 30 cycles of denaturation at 95°C for 30 s, annealing at 60°C for 30 s, and extension at 72°C for 3 min. The amplified products were separated by agarose gel electrophoresis and used for direct DNA sequencing. To establish the 5′ ends of the HCV transcripts from pHHJFH1, a synthetic 45-nt RNA adapter (Table 1) was ligated to RNA extracted from the transfected cells 1 day p.t. using T4 RNA ligase (Takara). The viral RNA sequences were then reverse transcribed using SuperScript III reverse transcriptase (Invitrogen) with a primer, RT (Table 1). The resultant cDNA sequences were subsequently amplified by PCR with 5′RACEouter-S and 5′RACEouter-R primers, followed by a second cycle of PCR using 5′RACEinner-S and 5′RACEinner-R primers (Table 1). To establish the terminal 3′-end sequences, extracted RNA sequences were polyadenylated using a poly(A) polymerase (Takara), reverse transcribed with CAC-T35 primer (Table 1), and amplified with the primers 3X-10S (Table 1) and CAC-T35. The amplified 5′ and 3′ cDNA sequences were then separated by agarose gel electrophoresis, cloned into the pGEM-T Easy vector (Promega), and sequenced.

Western blotting. The proteins were transferred onto a polyvinylidene difluoride membrane (Immobilon; Millipore, Bedford, MA) after separation by SDS-PAGE. After blocking, the membranes were probed with a mouse monoclonal anti-HCV core antibody (2H9) (49), a rabbit polyclonal anti-NS5B antibody, or a mouse monoclonal GAPDH (glyceraldehyde-3-phosphate dehydrogenase) antibody (Chemicon, Temecula, CA), followed by incubation with a peroxidase-conjugated secondary antibody and visualization with an ECL Plus Western blotting detection system (Amersham, Buckinghamshire, United Kingdom).

Quantification of HCV core protein. HCV core protein was quantified by using a highly sensitive enzyme immunoassay (Ortho HCV antigen ELISA kit; Ortho Clinical Diagnostics, Tokyo, Japan) in accordance with the manufacturer's instructions.

Sucrose density gradient analysis. Samples of cell culture supernatant were processed by low-speed centrifugation and passage through a 0.45-μm-pore-size filter. The filtrated supernatant was then concentrated ~30-fold by ultrafiltration by using an Amicon Ultra-15 filter device with a cutoff molecular mass of 100,000 kDa (Millipore), after which it was layered on top of a continuous 10 to 60% (wt/vol) sucrose gradient, followed by centrifugation at 35,000 rpm at 4°C for 14 h with an SW41 rotor (Beckman Coulter, Fullerton, CA). Fractions of 1 ml were collected from the bottom of the gradient. The core level and infectivity of HCV in each fraction were determined.

Quantification of HCV infectivity. Infectious virus titration was performed by a 50% tissue culture infectious dose ($TCID_{50}$) assay, as previously described (23, 26). Briefly, naive Huh7.5.1 cells were seeded at a density of 10^4 cells/well in a 96-well flat-bottom plate 24 h prior to infection. Five serial dilutions were performed, and the samples were used to infect the seeded cells (six wells per dilution). At 72 h after infection, the inoculated cells were fixed and immunostained with a rabbit polyclonal anti-NS5A antibody (14), followed by an Alexa Fluor 488-conjugated anti-rabbit secondary antibody (Invitrogen).

Labeling of *de novo*-synthesized viral RNA and immunofluorescence staining. Labeling of *de novo*-synthesized viral RNA was performed as previously described with some modifications (40). Briefly, cells were plated onto an eight-well chamber slide at a density of 5×10^4 cells/well. One day later, the cells were incubated with actinomycin D at a final concentration of 10 μg/ml for 1 h and washed twice with HEPES-saline buffer. Bromouridine triphosphate (BrUTP) at 2 mM was subsequently transfected into the cells using FuGENE 6 transfection reagent, after which the cells were incubated for 15 min on ice. After the cells were washed twice with phosphate-buffered saline (PBS), they were incubated in fresh DMEM supplemented with 10% FBS at 37°C for 4 h. The cells were then fixed with 4% paraformaldehyde for 20 min and permeabilized with PBS containing 0.1% Triton X-100 for 15 min at room temperature. Immunofluorescence staining of NS5A and *de novo*-synthesized HCV RNA was performed as previously described (26, 40). The nuclei were stained with DAPI (4′,6′-diamidino-2-phenylindole) solution (Sigma-Aldrich). Confocal microscopy was performed

TABLE 1. Oligonucleotides used for RT-PCR and RACE of the JFH-1 genome

Method or segment	Oligonucleotide	Sequences (5′–3′)
5′RACE	RT	GTACCCCATGAGGTCGGCAAAG
	45-nt RNA adapter	GCUGAUGGCGAUGAAUGAACACUGCGUUUGCUGGCUUUGAUGAAA
	5′RACEouter-S	GCTGATGGCGATGAATGAACACTG
	5′RACEouter-R	GACCGCTCCGAAGTTTTCCTTG
	5′RACEinner-S	GAACACTGCGTTTGCTGGCTTTGATG
	5′RACEinner-R	CGCCCTATCAGGCAGTACCACAAG
3′RACE	CAC-T35	CACTTTTTTTTTTTTTTTTTTTTTTTTTTTTTTTTT
	3X-10S	ATCTTAGCCCTAGTCACGGC
nt 129-2367	44S (1st PCR)	CTGTGAGGAACTACTGTCTT
	2445R	TCCACGATGTTCTGGTGAAG
	17S (2nd PCR)	CGGGAGAGCCATAGTGG
	2367R	CATTCCGTGGTAGAGTGCA
nt 2285-4665	2099S (1st PCR)	ACGGACTGTTTTAGGAAGCA
	4706R	TTGCAGTCGATCACGGAGTC
	2285S (2nd PCR)	AACTTCACTCGTGGGGATCG
	4665R	TCGGTGGCGACGACCAC
nt 4574-7002	4547S (1st PCR)	AAGTGTGACGAGCTCGCGG
	7027R	CATGAACAGGTTGGCATCCACCAT
	4594S (2nd PCR)	CGGGGTATGGGCTTGAACGC
	7003R	GTGGTGCAGGTGGCTCGCA
nt 6949-9634	6881S (1st PCR)	ATTGATGTCCATGCTAACAG
	3X-75R	TACGGCACTCTCTGCAGTCA
	6950S (2nd PCR)	GAGCTCCTCAGTGAGCCAG
	3X-54R	GCGGCTCACGGACCTTTCAC

using a Zeiss confocal laser scanning microscope LSM 510 (Carl Zeiss, Oberkochen, Germany).

Luciferase assay. Huh7.5.1 cells were seeded onto a 24-well cell culture plate at a density of 3×10^4 cells/well 24 h prior to inoculation with 100 μl of supernatant from the transfected cells. The cells were incubated for 72 h, followed by lysis with 100 μl of lysis buffer. The luciferase activity of the cells was determined by using a luciferase assay system (Promega). All luciferase assays were done at least in triplicate. For the neutralization experiments, a mouse monoclonal anti-CD81 antibody (JS-81; BD Pharmingen, Franklin Lakes, NJ) and a mouse monoclonal anti-FLAG antibody (Sigma-Aldrich) were used.

Flow cytometric analysis. Cells detached by treatment with trypsin were incubated in PBS containing 1% (vol/vol) formaldehyde for 15 min. A total of 5×10^5 cells were resuspended in PBS and treated with or without 0.75 μg of anti-CD81 antibody for 30 min at 4°C. After being washed with PBS, the cells were incubated with an Alexa Fluor 488-conjugated anti-mouse secondary antibody (Invitrogen) at 1:200 for 30 min at 4°C, washed repeatedly, and resuspended in PBS. Analyses were performed by using FACSCalibur system (Becton Dickinson, Franklin Lakes, NJ).

RESULTS

Analysis of the 5′ and 3′ ends of HCV RNA sequences generated from Pol I-driven plasmids. To examine whether the HCV transcripts generated from Pol I-driven plasmids had correct nucleotides at the 5′ and 3′ ends, we extracted RNA from Huh-7 cells transfected with pHHJFH1, which carries a genome-length HCV cDNA with a Pol I promoter/terminator, as well as from the culture supernatants. After this, the nucleotide sequences at both ends were determined using RACE and sequence analysis. A 328-nt fragment corresponding to cDNA from the 5′ end of HCV RNA was detected in the cell samples (Fig. 1A). Cloning of amplified fragments confirmed that the HCV transcripts were initiated from the first position of the viral genome in all of the clones sequenced (Fig. 1B). Similarly, a 127-nt amplification fragment was detected in each sample by 3′RACE (Fig. 1C), and the same 3′-end nucleotide sequence was observed in all clones derived from the culture supernatant (Fig. 1D, left). An additional two nucleotides (CC) were found at the 3′ end of the HCV transcript in a limited number of sequences (1 of 11 clones) derived from the cell sample (Fig. 1D, right), which were possibly derived from the Pol I terminator sequence by incorrect termination. These results indicate that most HCV transcripts generated from the Pol I-based HCV cDNA expression system are faithfully processed, although it is not determined whether the 5′ terminus of the viral RNA generated from Pol I system is triphosphate or monophosphate. It can be speculated that viral RNA lacking modifications at the 5′ and 3′ ends is preferentially packaged and secreted into the culture supernatant.

Production of HCV RNA, proteins, and virions from cells transiently transfected with Pol I-driven plasmids. To examine HCV RNA replication and protein expression in cells transfected with pHHJFH1, pHHJFH1/GND, or virion production-defective mutants, pHHJFH1/ΔE and pHHJFH1/R783A/R785A, which possess an in-frame deletion of E1/E2 region and substitutions in the p7 region, respectively (19, 42, 49), RPA and Western blotting were performed 5 days p.t. (Fig. 2A, B, and D). Positive-strand HCV RNA sequences were more abundant than negative-strand RNA sequences in these cells. Positive-strand RNA, but not negative-strand RNA, was detected in cells transfected with the replication-defective mutant pHHJFH1/GND (Fig. 2A and B). Northern blotting showed that genome-length RNA was generated in pHHJFH1-transfected cells but not in pHHJFH1/GND-transfected cells (Fig. 2C).

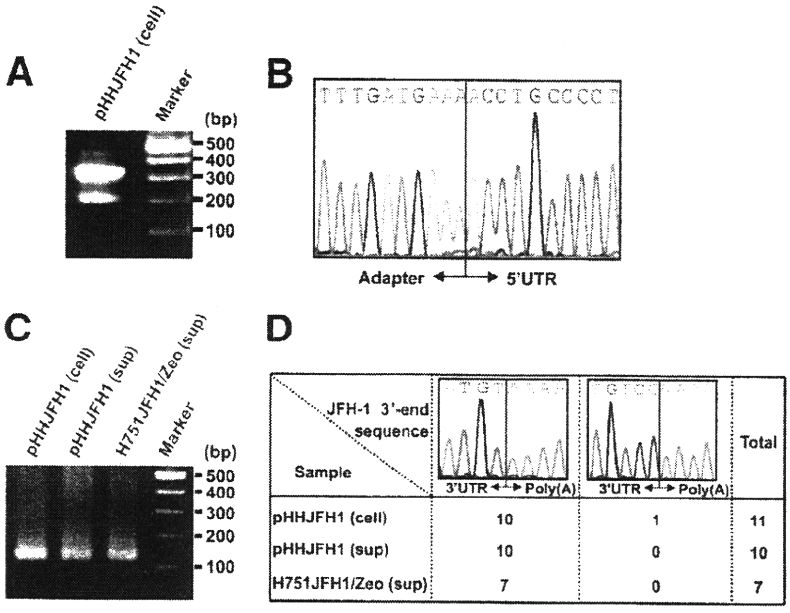

FIG. 1. Determination of the nucleotide sequences at the 5′-and 3′ ends of HCV RNA produced by the Pol I system. (A and B) 5′RACE and sequence analysis. A synthesized RNA adapter was ligated to RNA extracted from cells transfected with pHHJFH1. The positive-strand HCV RNA was reverse transcribed, and the resulting cDNA was amplified by nested PCR. The amplified 5′-end cDNA was separated by agarose gel electrophoresis (A), cloned, and sequenced (B). (C and D) 3′RACE and sequence analysis. RNA extracted from pHHJFH1-transfected cells, the culture supernatant of transfected cells, and the culture supernatant of H751JFH1/Zeo cells were polyadenylated, reverse transcribed, and amplified by PCR. The amplified 3′-end cDNA was separated by agarose gel electrophoresis (C), cloned, and sequenced (D).

As shown in Fig. 2D, the intracellular expression of core and NS5B proteins was comparable among cells transfected with pHHJFH1, pHHJFH1/ΔE, and pHHJFH1/R783A/R785A. Neither viral protein was detected in pHHJFH1/GND-transfected cells, suggesting that the level of viral RNA generated transiently from the DNA plasmid does not produce enough HCV proteins for detection and that ongoing amplification of the HCV RNA by the HCV NS5B polymerase allows a high enough level of viral RNA to produce detectable levels of HCV proteins.

To assess the release of HCV particles from cells transfected with Pol I-driven plasmids, core protein was quantified in culture supernatant by enzyme-linked immunosorbent assay (ELISA) or sucrose density gradient centrifugation. Core protein secreted from pHHJFH1-transfected cells was first detectable 2 days p.t., with levels increasing up to ~4 pmol/liter on day 6 (Fig. 3A). This core protein level was 4- to 6-fold higher than that in the culture supernatant of pHHJFH1/ΔE- or pHHJFH1/R783A/R785A-transfected cells, despite comparable intracellular core protein levels (Fig. 2D). Core protein was not secreted from cells transfected with pHHJFH1/GND (Fig. 3A). In another experiment, a plasmid expressing the secreted form of human placental alkaline phosphatase (SEAP) was cotransfected with each Pol I-driven plasmid. SEAP activity in culture supernatant was similar among all transfection groups, indicating comparable efficiencies of transfection (data not shown). Sucrose density gradient analysis of the concentrated supernatant of pHHJFH1-transfected cells indicated that the distribution of core protein levels peaked in the fraction of 1.17 g/ml density, while the peak of infectious titer was observed in the fraction of 1.12 g/ml density (Fig. 3B), which is consistent with the results of previous studies based on JFH-1-RNA transfection (23).

We next compared the kinetics of HCV particle secretion in the Pol I-driven system and RNA transfection system. Huh-7 cells, which have limited permissiveness for HCV infection (2), were transfected with either pHHJFH1 or JFH-1 RNA, and then cultured by passaging every 2 or 3 days. As shown in Fig. 3C, both methods of transfection demonstrated similar kinetics of core protein levels until 9 days p.t., after which levels gradually fell. However, significantly greater levels of core protein were detected in the culture of pHHJFH1-transfected cells compared to the RNA-transfected cells on day 12 and 15 p.t. This is likely due to an ongoing production of positive-strand viral RNA from transfected plasmids since RNA degradation generally occurs more quickly than that of circular DNA.

Establishment of stable cell lines constitutively producing HCV virion. To establish cell lines with constitutive HCV production, pHHJFH1/Zeo carrying HCV genomic cDNA and the Zeocin resistance gene were transfected into Huh7.5.1 cells. After approximately 3 weeks of culture with zeocin at a concentration of 0.4 mg/ml, cell colonies producing HCV core protein were screened by ELISA, and three clones were identified that constitutively produced the viral protein (H751JFH1/Zeo cells). Core protein levels within the culture supernatant of selected clones (H751-1, H751-6, and H751-50) were 2.0×10^4, 2.7×10^3, and 1.4×10^3 fmol/liter, respectively. Clone H751-1 was further analyzed. Indirect immunofluorescence with an anti-NS5A antibody showed fluorescent staining of NS5A in the cytoplasm of almost all H751JFH1/

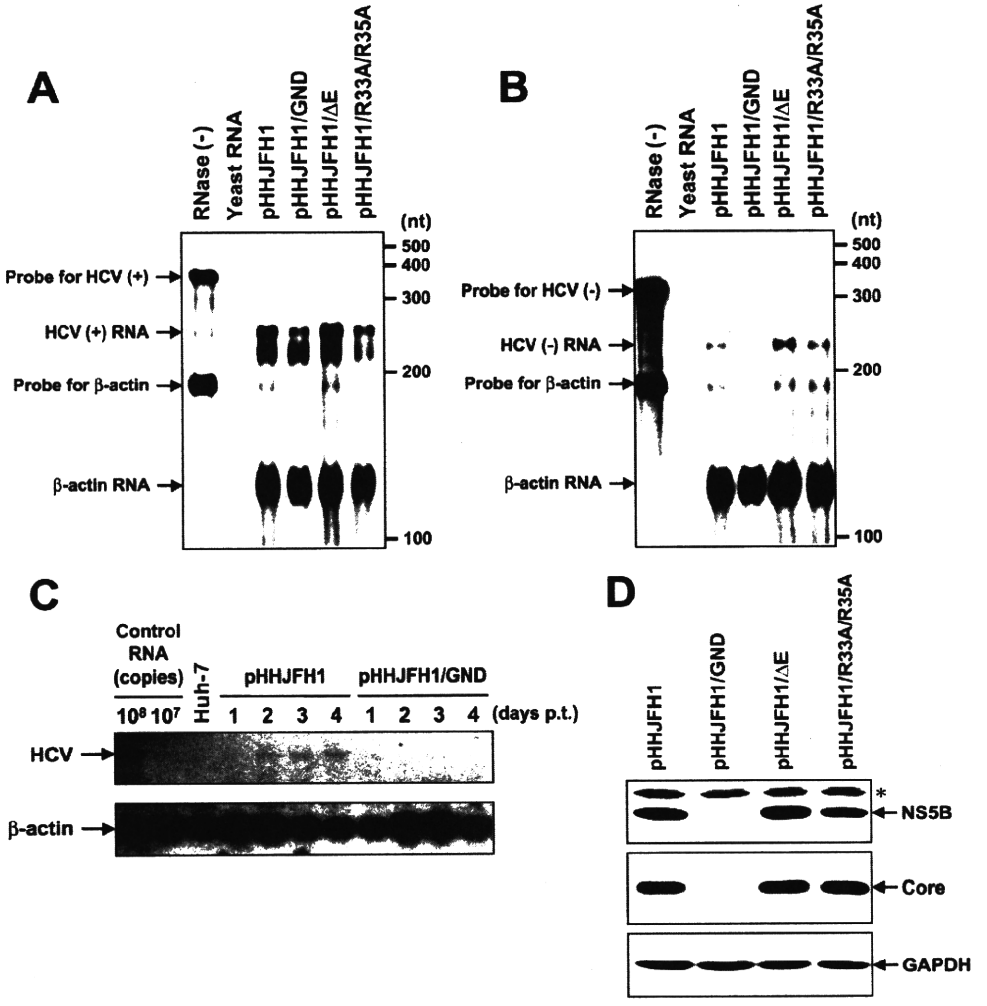

FIG. 2. HCV RNA replication and protein expression in cells transfected with Pol I-driven plasmids. (A and B) Assessment of HCV RNA replication by RPA. Pol I-driven HCV-expression plasmids were transfected into Huh-7 cells. Total RNA was extracted from the cells on day 5 p.t. and positive (A)- and negative (B)-strand HCV RNA levels were determined by RPA as described in Materials and Methods. In the RNase (−) lanes, yeast RNA mixed with RNA probes for HCV and human β-actin were loaded without RNase A/T1 treatment. In the yeast RNA lanes, yeast RNA mixed with RNA probes for HCV and human β-actin were loaded in the presence of RNase A/T1. (C) Northern blotting of total RNAs prepared from the transfected cells. Huh-7 cells transfected with pHHJFH1 or pHHJFH1/GND were harvested for RNA extraction through days 1 to 4 p.t. Control RNA, given numbers of synthetic HCV RNA; Huh-7, RNA extracted from naive cells. Arrows indicate full-length HCV RNA and β-actin RNA. (D) HCV protein expression in the transfected cells. Pol I-driven HCV-expression plasmids were transfected into Huh-7 cells, harvested, and lysed on day 6 p.t. The expression of NS5B, core, and GAPDH was analyzed by Western blotting as described in Materials and Methods. The asterisk indicates nonspecific bands.

Zeo cells (Fig. 4A), whereas no signal was detected in parental Huh7.5.1 cells (Fig. 4B). To determine where HCV RNA replicates in H751JFH1/Zeo cells, labeling of *de novo*-synthesized HCV RNA was performed. After interfering with mRNA production by exposure to actinomycin D, BrUTP-incorporated *de novo*-synthesized HCV RNA was detected in the cytoplasm of H751JFH1/Zeo cells (Fig. 4D) colocalized with NS5A in the perinuclear area (Fig. 4E and F).

Low mutation frequency of the viral genome in a long-term culture of H751JFH1/Zeo cells. The production level of infectious HCV from H751JFH1/Zeo cells at a concentration of $\sim 10^3$ $TCID_{50}$/ml was maintained over 1 year of culture (data not shown). It has been shown that both virus and host cells may adapt during persistent HCV infection in cell cultures, such that cells become resistant to infection due to reduced expression of the viral coreceptor CD81 (54). As shown in Fig. 5, we analyzed the cell surface expression of CD81 on the established cell lines by flow cytometry and observed markedly reduced expression on H751JFH1/Zeo cells compared to parental Huh7.5.1 cells. It is therefore possible that only a small proportion of HCV particles generated from H751JFH1/Zeo cells enter and propagate within the cells. The H751JFH1/Zeo system is thought to result in virtually a single cycle of HCV production from the chromosomally integrated gene and thus

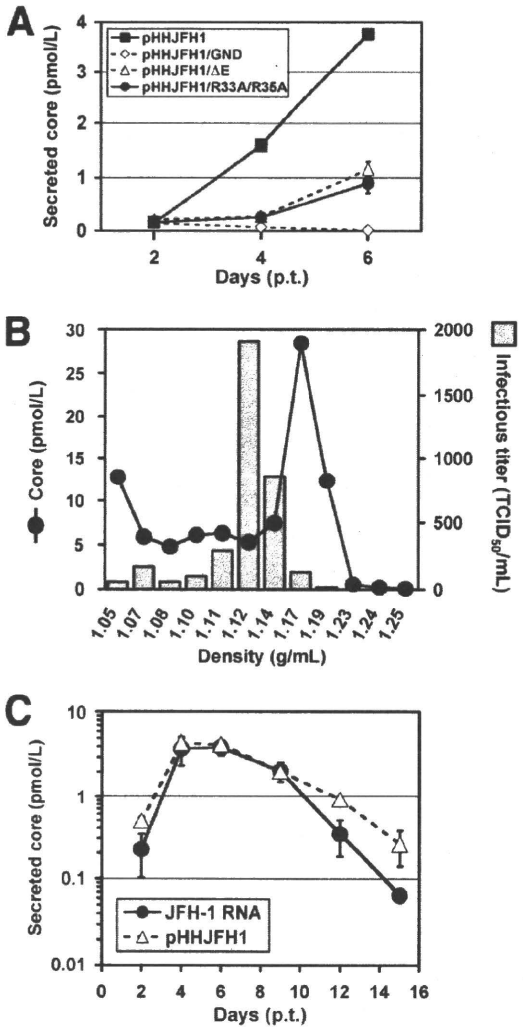

FIG. 3. HCV released from cells transfected with Pol I-driven plasmids. (A) HCV particle secretion from the transfected cells. The culture supernatant of Huh-7 cells transfected with Pol I-driven plasmids containing wild-type or mutated HCV genome were harvested on days 2, 4, and 6 and assayed for HCV core protein levels. The data for each experiment are averages of triplicate values with error bars showing standard deviations. (B) Sucrose density gradient analysis of the culture supernatant of pHHJFH1-transfected cells. Culture supernatant collected on day 5 p.t. was cleared by low-speed centrifugation, passed through a 0.45-μm-pore-size filter, and concentrated ~30-fold by ultrafiltration. After fractionating by sucrose density gradient centrifugation, the core protein level and viral infectious titer of each fraction were measured. (C) Kinetics of core protein secretion from cells transfected with pHHJFH1 or with JFH-1 genomic RNA. A total of 10^6 Huh-7 cells were transfected with 3 μg of pHHJFH1 or the same amount of *in vitro*-transcribed JFH-1 RNA by electroporation. The cells were passaged every 2 to 3 days before reaching confluence. Culture supernatant collected on the indicated days was used for core protein measurement. The level of secreted core protein (pmol/liter) is expressed on a logarithmic scale. The data for each experiment are averages of triplicate values with error bars showing standard deviations.

may yield a virus population with low mutation frequencies. To further examine this, we compared HCV genome mutation rates following production from H751JFH1/Zeo cells compared to cells constitutively infected with HCV after serial passages. RNAs were extracted from the supernatant of H751JFH1/Zeo cells cultured for 120 days, and cDNA sequences were amplified by nested PCR with four sets of primers encompassing almost the entire HCV genome (Table 1). PCR products with expected sizes of 2 to 2.5 kb were obtained [Fig. 6A, RT(+)] and subjected to direct sequencing. No amplified product was detected in samples without reverse transcription [Fig. 6A, RT(−)], suggesting no DNA contamination in culture supernatants or extracted RNA solutions. As shown in Fig. 5B (upper panel), three nucleotide mutations, including two substitutions in the E1 (nt 1218) and E2 (nt 1581) regions, and one deletion in the 3′ UTR (nt 9525) were found within the HCV genome with the mutation rate calculated at 9.6×10^{-4} base substitutions/site/year. These mutations were not detected in the chromosomally integrated HCV cDNA (data not shown). The present results also indicate that no splicing of the viral RNA occurred in the Pol I-based HCV JFH-1 expression system. The HCV genome sequence produced by JFH-1 virus-infected Huh7.5.1 cells was analyzed in the same way using culture supernatant 36 days after RNA transfection. As shown in Fig. 6B (lower panel), 10 mutations, including five substitutions throughout the open reading frame and five deletions in the 3′UTR, were detected, and the mutation rate was calculated at 1.1×10^{-2} base substitutions/site/year.

Effects of glycosylation inhibitors on HCV production. It is known that N-linked glycosylation and oligosaccharide trimming of a variety of viral envelope proteins including HCV E1 and E2 play key roles in the viral maturation and virion production. To evaluate the usefulness of the established cell line for antiviral testing, we determined the effects of glycosylation inhibitors, which have little to no cytotoxicity at the concentrations used, on HCV production in a three day assay using H751JFH1/Zeo cells. The compounds tested are known to inhibit the endoplasmic reticulum (ER), Golgi-resident glucosidases, or mannosidases that trim glucose or mannose residues from N-linked glycans. Some are reported to be involved in proteasome-dependent or -independent degradation of misfolded or unassembled glycoproteins to maintain protein integrity (4, 8, 27, 35).

As shown in Fig. 7A and B, treatment of H751JFH1/Zeo cells with increasing concentrations of *N*N-DNJ, which is an inhibitor of ER α-glucosidases, resulted in a dose-dependent reduction in secreted core protein. *N*N-DNJ was observed to have an IC_{50} (i.e., the concentration inhibiting 50% of core protein secretion) of ~20 μM. In contrast, KIF, which is an ER α-mannosidase inhibitor, resulted in a 1.5- to 2-fold increase in secreted core protein compared to control levels. The other five compounds did not significantly change core protein levels. We further determined the effects of *N*N-DNJ and KIF on the production of infectious HCV (Fig. 7C). As expected, *N*N-DNJ reduced the production of infectious virus in a dose-dependent manner, while production increased in the presence of KIF at 10 to 100 μM. Since *N*N-DNJ and KIF did not significantly influence viral RNA replication, as determined using the subgenomic replicon (data not shown), the present results suggest that some step(s), such as virion assembly, intracellular trafficking, and secretion, may be up- or downregulated depending on glycan modifications of HCV envelope proteins within the ER. Inhibitory effect of *N*N-DNJ was reproducibly observed using the cell line after 1 year of culturing

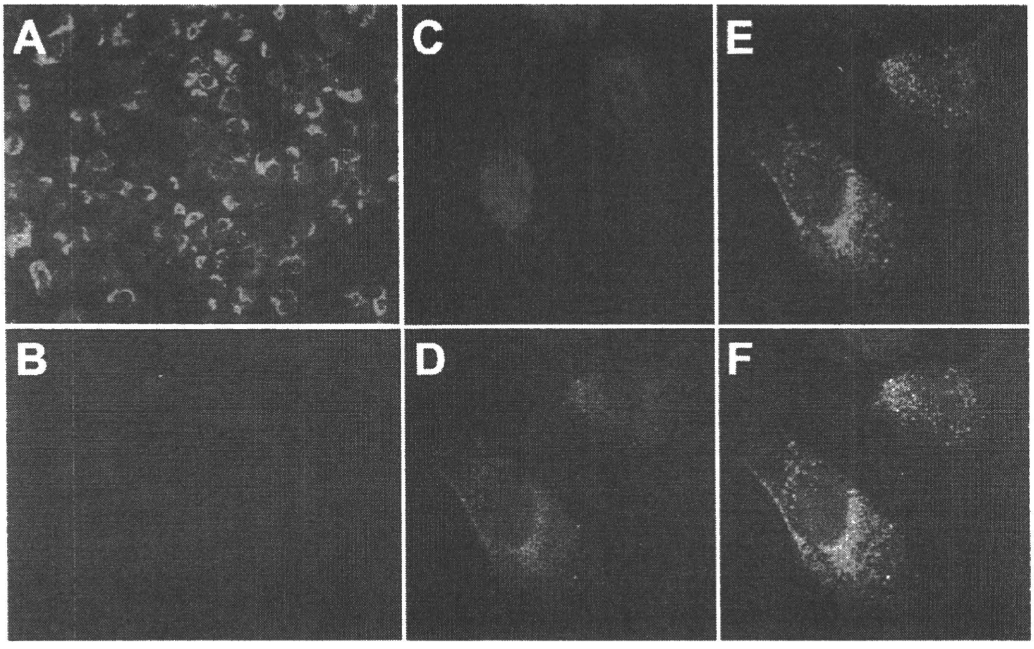

FIG. 4. Indirect immunofluorescence analysis of H751JFH1/Zeo cells. (A and B) H751JFH1/Zeo cells (A) and parental Huh7.5.1 cells (B) were immunostained with an anti-NS5A antibody. (C to F) The subcellular colocalization of *de novo*-synthesized HCV RNA and NS5A in H751JFH1/Zeo cells was analyzed. The cells were stained with DAPI (C), an anti-bromodeoxyuridine antibody (D), and an anti-NS5A antibody (E). The merge panel is shown in panel F.

(Fig. 7D). Under the same condition, the core protein secretion was inhibited by 28 and 58% with 10 and 100 nM BILN 2061, an NS3 protease inhibitor, respectively (Fig. 7D).

Replicon *trans*-packaging system. Recently, ourselves and others have developed a packaging system for HCV subgenomic replicon RNA sequences by providing *trans* viral core-NS2 proteins (1, 17, 41). Since viral structural proteins are not encoded by the subgenomic replicon, progeny virus cannot be produced after transfection. Thus, the single-round infectious HCV-like particle (HCV-LP) generated by this system potentially improves the safety of viral transduction. Here, in order to make the *trans*-packaging system easier to manipulate, we used a Pol I-driven plasmid to develop a transient two-plasmid expression system for the production of HCV-LP. pHH/SGR-Luc, which carries a bicistronic subgenomic reporter replicon with a Pol I promoter/terminator, or its replication-defective mutant, were cotransfected with or without a core-NS2 expression plasmid (Fig. 8A). The culture supernatant was then collected between days 2 and 5 p.t. and used to inoculate naive Huh7.5.1 cells. Reporter luciferase activity, as a quantitative measure of infectious virus production, was assessed in the cells 3 days postinoculation. As shown in Fig. 8B, reporter replication activity was easily detectable in cells inoculated with culture supernatant from cells cotransfected with pHH/

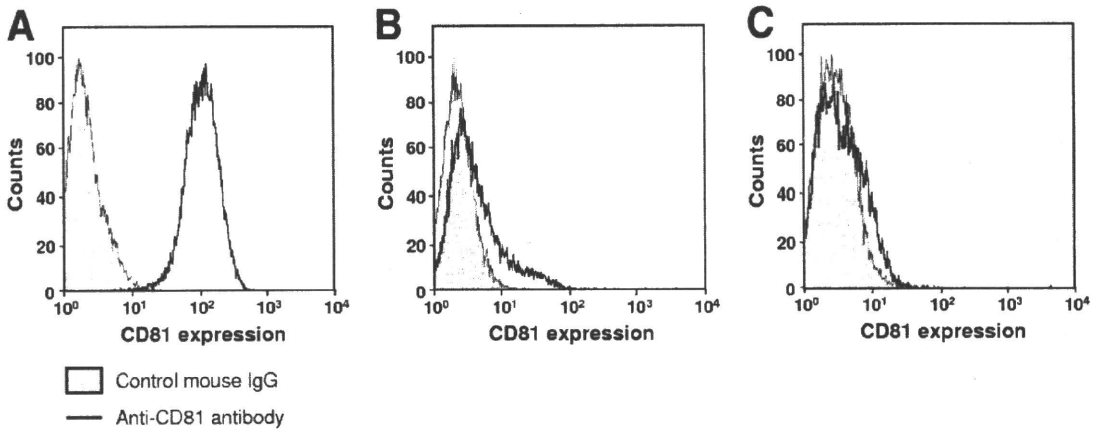

FIG. 5. Loss of CD81 expression in H751JFH1/Zeo cells. The cell surface expression of CD81 on Huh7.5.1 cells (A), H751JFH1/Zeo clone H751-1 (B), and clone H751-50 (C) was analyzed by flow cytometry after being stained with anti-CD81 antibody.

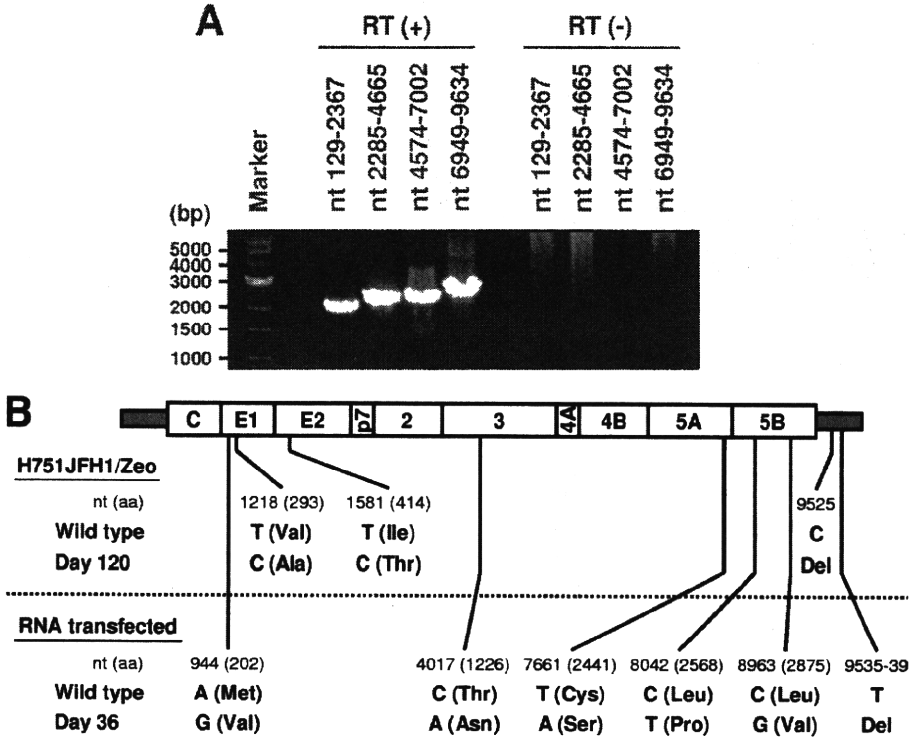

FIG. 6. Genome mutations of HCV secreted from H751JFH1/Zeo cells. (A) RT-PCR of HCV genome extracted from the culture supernatant of H751JFH1/Zeo cells. Viral RNA sequences were reverse transcribed [RT (+)] or not [RT (−)], followed by amplification with primer pairs encompassing the specified HCV genome regions. (B) Comparison of the genome mutations of HCV secreted from H751JFH1/Zeo cells cultured for 120 days (upper panel) and JFH-1 RNA-transfected cells cultured for 36 days (lower panel). The positions of original (wild-type) and mutated (day 120, day 36) nucleotides are indicated under the schematic diagram of the HCV genome. Amino acid residues and their positions are marked in parentheses. Del, deletion.

SGR-Luc and pCAG/C-NS2, with an ~10-fold increase in activity observed at 2 to 5 days p.t. In contrast, luciferase signal in the Huh7.5.1 cells inoculated from supernatant of cells transfected with pHH/SGR-Luc with polymerase-deficient mutation (GND) showed background levels. There was a faint luciferase signal in the cells inoculated from supernatant of cells transfected with pHH/SGR-Luc in the absence of pCAG/C-NS2, suggesting carryover of a low level of cells with the supernatants. Transfer of supernatant from infected cells to naive Huh7.5.1 cells did not result in infection, as judged by undetectable luciferase activity (data not shown). To examine whether NS2 is important for HCV production as previously demonstrated (17–19, 52), we compared the expression of core-NS2 versus core-p7 in the packaged cells (Fig. 8C). The reporter activity in cells inoculated with virus *trans*-packaged by core-p7 was ~100-fold lower than the virus *trans*-packaged by core-NS2, indicating that NS2 needs to be expressed with the structural proteins for efficient assembly and/or infectivity. CD81-dependent infection of HCV-LP was further confirmed by demonstrating reduced reporter activity in the presence of anti-CD81 antibody (Fig. 8D). Thus, we developed a simple *trans*-encapsidation system based on transient two-plasmid transfection, which permits experimental separation of HCV genome replication and virion assembly.

DISCUSSION

Here, we exploited Pol I-derived vectors for expression of the HCV genome, a strategy that generates viral RNAs from the Pol I promoter and terminator. We demonstrated that the HCV JFH-1 RNA produced using this system is unspliced with precise sequences at both ends and that it is replicated in the cytoplasm of transfected cells to produce infectious particles. This approach was used to establish a replicon *trans*-packaging system based on transient two-plasmid transfection and enables the production of a stable cell line capable of constitutive HCV production. The cell line produced using this method can be used to screen a large number of potential antiviral agents by assessing their ability to interfere with HCV replication and/or virion formation. The Pol I-mediated transcription system was originally developed to perform reverse genetics on influenza A viruses (12, 29) which replicate in the nucleus. This system has also been shown useful in the development of reverse genetics for negative-strand RNA viruses having a cytoplasmic replication cycle (3, 10, 11, 31). The results of the present study suggest that the Pol I system can also be used to perform reverse genetics on a cytoplasmically replicating positive-strand RNA virus.

Although viral RNA transfection by electroporation is the most commonly used method to perform reverse genetics on

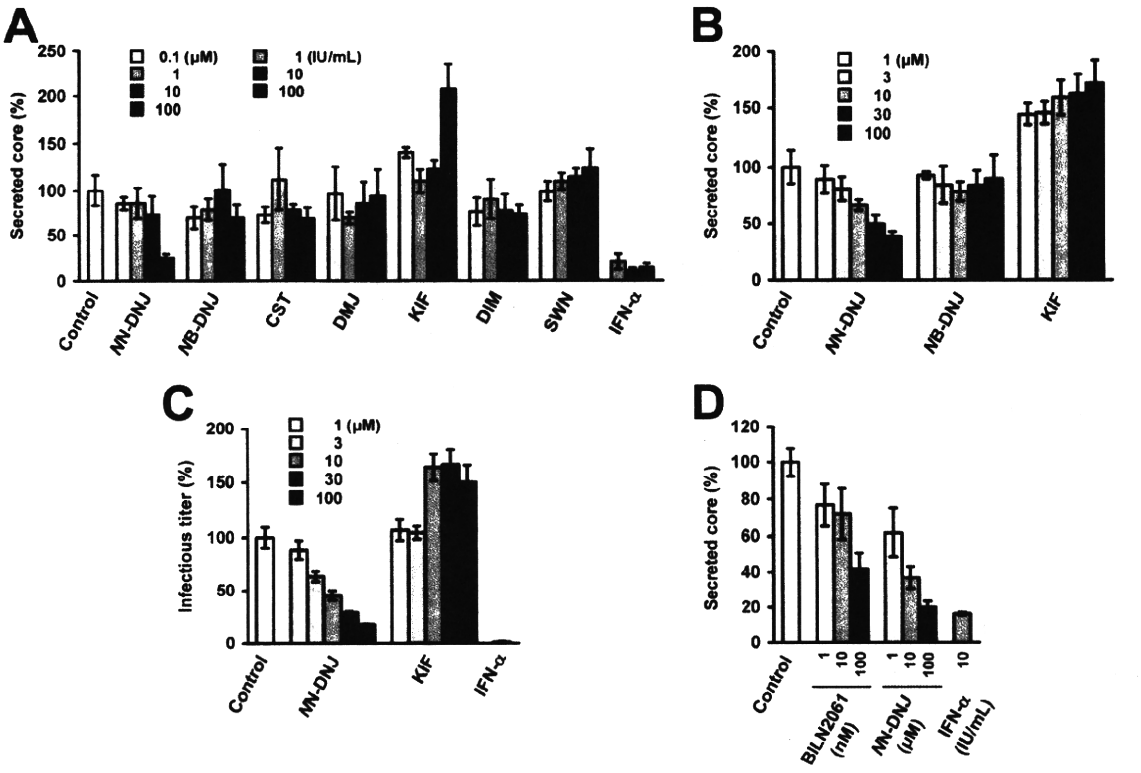

FIG. 7. Effects of glycosylation inhibitors on HCV production from H751JFH1/Zeo cells. (A and B) Effects of glycosylation inhibitors on the secretion of HCV core protein. H751JFH1/Zeo cells were seeded at a density of 1×10^4 cells/well in a 96-well culture plate (A) or 3×10^4 cells/well in a 12-well cell culture plate (B). One day later, each compound was added to the cell culture supernatant at the indicated concentrations. The culture supernatant was collected after a further 3-day culture and processed by core protein-specific ELISA. The control represents an untreated cell culture. The level of secreted core protein was normalized by setting the control value at 100%. The data for each experiment are averages of triplicate values with error bars showing standard deviations. (C) Effects of *N*N-DNJ and KIF on infectious HCV production. The culture supernatant obtained in panel B was used to infect naive Huh7.5.1 cells. At 72 h after infection, the inoculated cells were fixed and immunostained as described in Materials and Methods for titration of virus infectivity. The infectious titer was normalized by setting the control value at 100%. Cells were treated with INF-α at 100 IU/ml as a positive control. The data for each experiment are averages of triplicate values with error bars showing standard deviations. The control represents an untreated cell culture. (D) After 1 year of culturing H751JFH1/Zeo cells, antiviral effects of *N*N-DNJ and BILN 2061 were evaluated. H751JFH1/Zeo cells were seeded at a density of 3×10^4 cells/well in a 12-well cell culture plate. One day later, each compound was added to the cell culture supernatant at the indicated concentrations. The culture supernatant was collected after a further 3-day culture and processed by core protein-specific ELISA. The control represents an untreated cell culture. The level of secreted core protein was normalized by setting the control value at 100%. The data for each experiment are averages of triplicate values with error bars showing standard deviations.

HCV (23, 49, 53), it is comparatively difficult to manipulate. RNA electroporation requires high-quality *in vitro*-synthesized RNA and a large quantity of exponential-growth-phase cells, which may be hard to provide when a number of different RNA constructs are being examined in the same experiment. In addition to the Pol I system, other DNA expression systems have been examined with regard to HCV particle production (5, 15, 21). These systems require ribozyme sequences to be inserted at either end of the HCV genomic cDNA sequence in order to generate appropriately processed viral RNA. However, Heller et al. have reported that the HCV RNA generated by *in vitro* transcription of a HCV-ribozyme plasmid contains uncleaved or prematurely terminated forms of HCV RNA. These authors have also demonstrated that HCV RNA from the culture supernatant of HCV-ribozyme plasmid-transfected cells possesses nucleotide changes at the 5′ and 3′ ends (15), suggesting that the ribozyme is less reliable at generating correct transcripts compared to our Pol I system. In fact, there is evidence to suggest that a mouse Pol I terminator is significantly more effective than an HDV ribozyme in generating precise 3′ ends of RNA, as demonstrated in a plasmid-based influenza virus rescue system (9). Recently, it has been demonstrated that Pol I-catalyzed rRNA transcription is activated in Huh-7 cells following infection with JFH-1 or transfection with a subgenomic HCV replicon (34). HCV NS5A has been shown to upregulate the transcription of Pol I, but not Pol II, through phosphorylation of an upstream binding factor, a Pol I DNA binding transcription factor. These observations indicate that a Pol I-mediated expression system is suitable for efficient production of infectious HCV by DNA transfection.

We established a stable cell line, H751JFH1/Zeo, that constitutively and efficiently produced infectious HCV particles by introducing a Pol I-driven plasmid containing a selection marker into Huh7.5.1 cells. Interestingly, the established cell

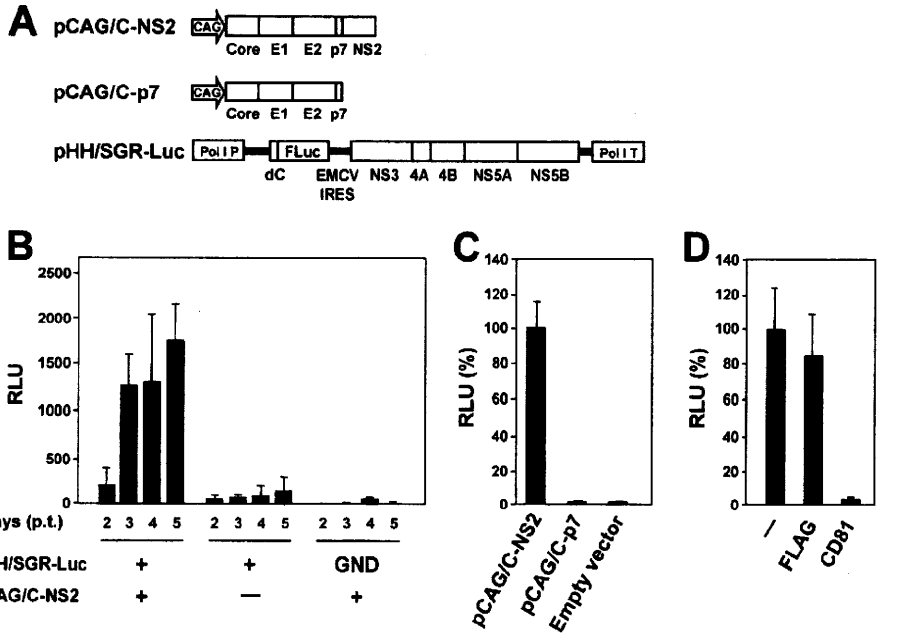

FIG. 8. Establishment of a *trans*-packaging system involving two-plasmid transfection. (A) Schematic representation of the plasmids used for the production of HCV-LP. HCV polyproteins are indicated by the open boxes. Bold lines indicate the HCV UTR. EMCV IRES is denoted by gray bars. The firefly luciferase gene (F Luc) is depicted as a gray box. CAG, CAG promoter; Pol I P, Pol I promoter; dC, 5′ region of Core gene; Pol I T, Pol I terminator. (B) Luciferase activity in Huh7.5.1 cells inoculated with culture supernatant from cells transfected with the indicated plasmids. Luciferase activity is expressed in terms of relative luciferase units (RLU). The data for each experiment are averages of triplicate values with error bars showing standard deviations. (C) Culture supernatant from cells cotransfected with pHH/SGR-Luc and the indicated plasmids were collected 4 days p.t. The luciferase activity in Huh7.5.1 cells inoculated with culture supernatant was determined 3 days postinoculation and expressed as relative luciferase units (RLU). The RLU was normalized according to the luciferase activity observed in the pCAG/C-NS2-transfected sample (C-NS2), which was set at 100%. The data for each experiment are averages of triplicate values with error bars showing standard deviations. (D) Huh7.5.1 cells were inoculated with HCVLP in the absence (−) or presence of 5 μg of anti-CD81 or anti-FLAG antibody/ml. The luciferase activity was determined 72 h postinoculation and is expressed as relative luciferase units (RLU). The RLU was normalized to the level of luciferase activity observed in the antibody-untreated sample (−), which was set at 100%. The data for each experiment are averages of triplicate values with error bars showing standard deviations.

clones exhibited little to no surface expression of CD81, one of the key features of HCV glycoprotein-mediated infection (Fig. 5). Defective expression of receptor molecules might be advantageous in generating stable cell lines for robust production of HCV. HCV-induced cytotoxicity has been reported (7, 45, 54). Persistent HCV infection was established after electroporation of JFH-1 genomic RNA, and a variable cytopathic effect was observed at the peak of acute HCV infection, as well as during the persistent phase of infection (54). A recent study has demonstrated that the cytopathic effect triggered by HCV RNA transfection and viral infection is characterized by massive apoptotic cell death with expression of several ER stress markers, such as GRP78 and phosphorylated eIF2-α (39). Therefore, in the present study, it is likely that selective forces to evade cell death during high levels of HCV replication produced cell populations resistant to virus infection. As a consequence, H751JFH1/Zeo cells maintained robust production of infectious HCV particles over a long period of time without gross cytopathic effects or changes in cell morphology.

Substantial evidence demonstrates that the mutation rate of the HCV genome produced in H751JFH1/Zeo was low (Fig. 6) presumably because of consistent expression of wild-type HCV RNA from the chromosomally integrated gene. Nevertheless, a considerable proportion of the genome was mutated, with two nonsynonymous mutations in the E1 (V293A) and E2 (I414T) regions identified in the culture supernatant of H751JFH1/Zeo cells after 4 months of passages (Fig. 6). A I414T mutation has also been reported after long-term propagation of HCV in culture after JFH-1-RNA transfection (54). This mutation is located between the hypervariable regions 1 and 2 within the N terminus of E2 (51). Adaptive mutations in this region have been shown to enhance virus expansion, presumably by enabling more efficient virus entry (6, 36, 54). A possible CD81-independent mechanism for cell-to-cell transmission of HCV has been proposed (48, 50). However, the mechanisms governing cell-to-cell spread of HCV are not well understood. Further investigation into the importance of envelope protein mutations in HCV transmission independent of CD81 provide a better understanding of the complex interactions required for HCV infection.

In the present study we assessed the effects of N-linked glycosylation inhibitors on HCV production using H751JFH1/Zeo (Fig. 7) and found that an α-glucosidase inhibitor *N*N-DNJ inhibits the production of infectious HCV, which has also been observed in previous studies (43, 47). In contrast, HCV production is increased in the presence of an ER α-mannosidase inhibitor KIF, but not in the presence of the Golgi α-mannosidase inhibitors DMJ, DIM, and SWN. KIF inhibits α-man-

nosidase I, which primarily functions to remove the middle mannose branch from $Man_9GlcNAc_2$ to form $Man_8GlcNAc_2$ after the removal of glucose residues by glucosidases I and II (8, 24). Experiments to elucidate the role of mannose trimming of N-glycans in the HCV life cycle are currently under way.

It has recently been demonstrated that subgenomic replicons or defective genomes of HCV that have the potential of translation and self-replication can be encapsidated into infectious viruslike particles by *trans*-complementation of the viral structural proteins (1, 17, 32, 41, 44). In these studies, the viral RNAs were generally generated by *in vitro* transcription from linearized corresponding plasmids, followed by electroporation into the cells. Structural proteins or Core to NS2 proteins were then provided by DNA or RNA transfection, viral-vector-based transduction, or stable packaging cell lines established. Here, we achieved the replicon *trans*-encapsidation via transient cotransfection with two DNA plasmids. This system, which is apparently easier to manipulate and allows production of *trans*-encapsidated materials more rapidly compared to the systems published, can be applied to the study for understanding phenomenon and biological significance of a variety of naturally occurring HCV subgenomic deletion variants that possibly circulate in hepatitis C patients.

In summary, we have established a Pol I-based reverse-genetics system for the efficient production of infectious HCV. This methodology can be applied to develop (i) a stable HCV-producing cell line with a low mutation frequency of the viral genome and (ii) a simple *trans*-encapsidation system with the flexibility of genome packaging and improved biosafety. This may be useful for antiviral screening and may assist in the development of a live-attenuated HCV vaccine.

ACKNOWLEDGMENTS

We are grateful to Francis V. Chisari (The Scripps Research Institute) for providing Huh7.5.1 cells and to Y. Kawaoka (School of Veterinary Medicine, University of Wisconsin-Madison) for providing the pHH21 vector. We thank A. Murayama and T. Date for their help in sequence and Northern blot analyses and our coworkers for their helpful discussions. We also thank S. Yoshizaki, T. Shimoji, M. Kaga, and M. Sasaki for their technical assistance and T. Mizoguchi for secretarial work.

This study was supported by grants-in-aid from the Ministry of Health, Labor, and Welfare; by the Program for Promotion of Fundamental Studies in Health Sciences of the Organization for Drug ADR Relief, R&D Promotion, and Product Review of Japan (01-3); and by Research on Health Sciences focusing on Drug Innovation from the Japan Health Sciences Foundation, Japan.

REFERENCES

1. **Adair, R., A. H. Patel, L. Corless, S. Griffin, D. J. Rowlands, and C. J. McCormick.** 2009. Expression of hepatitis C virus (HCV) structural proteins in trans facilitates encapsidation and transmission of HCV subgenomic RNA. J. Gen. Virol. **90**:833–842.
2. **Akazawa, D., T. Date, K. Morikawa, A. Murayama, M. Miyamoto, M. Kaga, H. Barth, T. F. Baumert, J. Dubuisson, and T. Wakita.** 2007. CD81 expression is important for the permissiveness of Huh7 cell clones for heterogeneous hepatitis C virus infection. J. Virol. **81**:5036–5045.
3. **Billecocq, A., N. Gauliard, N. Le May, R. M. Elliott, R. Flick, and M. Bouloy.** 2008. RNA polymerase I-mediated expression of viral RNA for the rescue of infectious virulent and avirulent Rift Valley fever viruses. Virology **378**:377–384.
4. **Cabral, C. M., P. Choudhury, Y. Liu, and R. N. Sifers.** 2000. Processing by endoplasmic reticulum mannosidases partitions a secretion-impaired glycoprotein into distinct disposal pathways. J. Biol. Chem. **275**:25015–25022.
5. **Cai, Z., C. Zhang, K. S. Chang, J. Jiang, B. C. Ahn, T. Wakita, T. J. Liang, and G. Luo.** 2005. Robust production of infectious hepatitis C virus (HCV) from stably HCV cDNA-transfected human hepatoma cells. J. Virol. **79**: 13963–13973.
6. **Delgrange, D., A. Pillez, S. Castelain, L. Cocquerel, Y. Rouille, J. Dubuisson, T. Wakita, G. Duverlie, and C. Wychowski.** 2007. Robust production of infectious viral particles in Huh-7 cells by introducing mutations in hepatitis C virus structural proteins. J. Gen. Virol. **88**:2495–2503.
7. **Deng, L., T. Adachi, K. Kitayama, Y. Bungyoku, S. Kitazawa, S. Ishido, I. Shoji, and H. Hotta.** 2008. Hepatitis C virus infection induces apoptosis through a Bax-triggered, mitochondrion-mediated, caspase 3-dependent pathway. J. Virol. **82**:10375–10385.
8. **Ellgaard, L., M. Molinari, and A. Helenius.** 1999. Setting the standards: quality control in the secretory pathway. Science **286**:1882–1888.
9. **Feng, L., F. Li, X. Zheng, W. Pan, K. Zhou, Y. Liu, H. He, and L. Chen.** 2009. The mouse Pol I terminator is more efficient than the hepatitis delta virus ribozyme in generating influenza-virus-like RNAs with precise 3′ ends in a plasmid-only-based virus rescue system. Arch. Virol. **154**:1151–1156.
10. **Flick, R., K. Flick, H. Feldmann, and F. Elgh.** 2003. Reverse genetics for Crimean-Congo hemorrhagic fever virus. J. Virol. **77**:5997–6006.
11. **Flick, R., and R. F. Pettersson.** 2001. Reverse genetics system for Uukuniemi virus (*Bunyaviridae*): RNA polymerase I-catalyzed expression of chimeric viral RNAs. J. Virol. **75**:1643–1655.
12. **Fodor, E., L. Devenish, O. G. Engelhardt, P. Palese, G. G. Brownlee, and A. Garcia-Sastre.** 1999. Rescue of influenza A virus from recombinant DNA. J. Virol. **73**:9679–9682.
13. **Groseth, A., H. Feldmann, S. Theriault, G. Mehmetoglu, and R. Flick.** 2005. RNA polymerase I-driven minigenome system for Ebola viruses. J. Virol. **79**:4425–4433.
14. **Hamamoto, I., Y. Nishimura, T. Okamoto, H. Aizaki, M. Liu, Y. Mori, T. Abe, T. Suzuki, M. M. Lai, T. Miyamura, K. Moriishi, and Y. Matsuura.** 2005. Human VAP-B is involved in hepatitis C virus replication through interaction with NS5A and NS5B. J. Virol. **79**:13473–13482.
15. **Heller, T., S. Saito, J. Auerbach, T. Williams, T. R. Moreen, A. Jazwinski, B. Cruz, N. Jeurkar, R. Sapp, G. Luo, and T. J. Liang.** 2005. An in vitro model of hepatitis C virion production. Proc. Natl. Acad. Sci. U. S. A. **102**:2579–2583.
16. **Hoofnagle, J. H.** 2002. Course and outcome of hepatitis C. Hepatology **36**:S21–S29.
17. **Ishii, K., K. Murakami, S. S. Hmwe, B. Zhang, J. Li, M. Shirakura, K. Morikawa, R. Suzuki, T. Miyamura, T. Wakita, and T. Suzuki.** 2008. Trans-encapsidation of hepatitis C virus subgenomic replicon RNA with viral structure proteins. Biochem. Biophys. Res. Commun. **371**:446–450.
18. **Jirasko, V., R. Montserret, N. Appel, A. Janvier, L. Eustachi, C. Brohm, E. Steinmann, T. Pietschmann, F. Penin, and R. Bartenschlager.** 2008. Structural and functional characterization of nonstructural protein 2 for its role in hepatitis C virus assembly. J. Biol. Chem. **283**:28546–28562.
19. **Jones, C. T., C. L. Murray, D. K. Eastman, J. Tassello, and C. M. Rice.** 2007. Hepatitis C virus p7 and NS2 proteins are essential for production of infectious virus. J. Virol. **81**:8374–8383.
20. **Kato, T., T. Date, M. Miyamoto, M. Sugiyama, Y. Tanaka, E. Orito, T. Ohno, K. Sugihara, I. Hasegawa, K. Fujiwara, K. Ito, A. Ozasa, M. Mizokami, and T. Wakita.** 2005. Detection of anti-hepatitis C virus effects of interferon and ribavirin by a sensitive replicon system. J. Clin. Microbiol. **43**:5679–5684.
21. **Kato, T., T. Matsumura, T. Heller, S. Saito, R. K. Sapp, K. Murthy, T. Wakita, and T. J. Liang.** 2007. Production of infectious hepatitis C virus of various genotypes in cell cultures. J. Virol. **81**:4405–4411.
22. **Liang, T. J., B. Rehermann, L. B. Seeff, and J. H. Hoofnagle.** 2000. Pathogenesis, natural history, treatment, and prevention of hepatitis C. Ann. Intern. Med. **132**:296–305.
23. **Lindenbach, B. D., M. J. Evans, A. J. Syder, B. Wolk, T. L. Tellinghuisen, C. C. Liu, T. Maruyama, R. O. Hynes, D. R. Burton, J. A. McKeating, and C. M. Rice.** 2005. Complete replication of hepatitis C virus in cell culture. Science **309**:623–626.
24. **Liu, Y., P. Choudhury, C. M. Cabral, and R. N. Sifers.** 1999. Oligosaccharide modification in the early secretory pathway directs the selection of a misfolded glycoprotein for degradation by the proteasome. J. Biol. Chem. **274**: 5861–5867.
25. **Manns, M. P., H. Wedemeyer, and M. Cornberg.** 2006. Treating viral hepatitis C: efficacy, side effects, and complications. Gut **55**:1350–1359.
26. **Masaki, T., R. Suzuki, K. Murakami, H. Aizaki, K. Ishii, A. Murayama, T. Date, Y. Matsuura, T. Miyamura, T. Wakita, and T. Suzuki.** 2008. Interaction of hepatitis C virus nonstructural protein 5A with core protein is critical for the production of infectious virus particles. J. Virol. **82**:7964–7976.
27. **Meusser, B., C. Hirsch, E. Jarosch, and T. Sommer.** 2005. ERAD: the long road to destruction. Nat. Cell Biol. **7**:766–772.
28. **Neumann, G., and Y. Kawaoka.** 2001. Reverse genetics of influenza virus. Virology **287**:243–250.
29. **Neumann, G., T. Watanabe, H. Ito, S. Watanabe, H. Goto, P. Gao, M. Hughes, D. R. Perez, R. Donis, E. Hoffmann, G. Hobom, and Y. Kawaoka.** 1999. Generation of influenza A viruses entirely from cloned cDNAs. Proc. Natl. Acad. Sci. U. S. A. **96**:9345–9350.
30. **Niwa, H., K. Yamamura, and J. Miyazaki.** 1991. Efficient selection for high-expression transfectants with a novel eukaryotic vector. Gene **108**:193–199.
31. **Ogawa, Y., K. Sugiura, K. Kato, Y. Tohya, and H. Akashi.** 2007. Rescue of

Akabane virus (family *Bunyaviridae*) entirely from cloned cDNAs by using RNA polymerase I. J. Gen. Virol. **88**:3385–3390.
32. **Pacini, L., R. Graziani, L. Bartholomew, R. De Francesco, and G. Paonessa.** 2009. Naturally occurring hepatitis C virus subgenomic deletion mutants replicate efficiently in Huh-7 cells and are trans-packaged in vitro to generate infectious defective particles. J. Virol. **83**:9079–9093.
33. **Poynard, T., M. F. Yuen, V. Ratziu, and C. L. Lai.** 2003. Viral hepatitis C. Lancet **362**:2095–2100.
34. **Raychaudhuri, S., V. Fontanes, B. Barat, and A. Dasgupta.** 2009. Activation of rRNA transcription by hepatitis C virus involves upstream binding factor phosphorylation via induction of cyclin D1. Cancer Res. **69**:2057–2064.
35. **Ruddock, L. W., and M. Molinari.** 2006. N-glycan processing in ER quality control. J. Cell Sci. **119**:4373–4380.
36. **Russell, R. S., J. C. Meunier, S. Takikawa, K. Faulk, R. E. Engle, J. Bukh, R. H. Purcell, and S. U. Emerson.** 2008. Advantages of a single-cycle production assay to study cell culture-adaptive mutations of hepatitis C virus. Proc. Natl. Acad. Sci. U. S. A. **105**:4370–4375.
37. **Seeff, L. B., and J. H. Hoofnagle.** 2003. Appendix: National Institutes of Health Consensus Development Conference Management of Hepatitis C 2002. Clin. Liver Dis. **7**:261–287.
38. **Seeff, L. B., and J. H. Hoofnagle.** 2002. National Institutes of Health Consensus Development Conference: management of hepatitis C: 2002. Hepatology **36**:S1–S2.
39. **Sekine-Osajima, Y., N. Sakamoto, K. Mishima, M. Nakagawa, Y. Itsui, M. Tasaka, Y. Nishimura-Sakurai, C. H. Chen, T. Kanai, K. Tsuchiya, T. Wakita, N. Enomoto, and M. Watanabe.** 2008. Development of plaque assays for hepatitis C virus-JFH1 strain and isolation of mutants with enhanced cytopathogenicity and replication capacity. Virology **371**:71–85.
40. **Shi, S. T., K. J. Lee, H. Aizaki, S. B. Hwang, and M. M. Lai.** 2003. Hepatitis C virus RNA replication occurs on a detergent-resistant membrane that cofractionates with caveolin-2. J. Virol. **77**:4160–4168.
41. **Steinmann, E., C. Brohm, S. Kallis, R. Bartenschlager, and T. Pietschmann.** 2008. Efficient trans-encapsidation of hepatitis C virus RNAs into infectious virus-like particles. J. Virol. **82**:7034–7046.
42. **Steinmann, E., F. Penin, S. Kallis, A. H. Patel, R. Bartenschlager, and T. Pietschmann.** 2007. Hepatitis C virus p7 protein is crucial for assembly and release of infectious virions. PLoS Pathog. **3**:e103.
43. **Steinmann, E., T. Whitfield, S. Kallis, R. A. Dwek, N. Zitzmann, T. Pietschmann, and R. Bartenschlager.** 2007. Antiviral effects of amantadine and iminosugar derivatives against hepatitis C virus. Hepatology **46**:330–338.
44. **Sugiyama, K., K. Suzuki, T. Nakazawa, K. Funami, T. Hishiki, K. Ogawa, S. Saito, K. W. Shimotohno, T. Suzuki, Y. Shimizu, R. Tobita, M. Hijikata, H. Takaku, and K. Shimotohno.** 2009. Genetic analysis of hepatitis C virus with defective genome and its infectivity in vitro. J. Virol. **83**:6922–6928.
45. **Sung, V. M., S. Shimodaira, A. L. Doughty, G. R. Picchio, H. Can, T. S. Yen, K. L. Lindsay, A. M. Levine, and M. M. Lai.** 2003. Establishment of B-cell lymphoma cell lines persistently infected with hepatitis C virus in vivo and in vitro: the apoptotic effects of virus infection. J. Virol. **77**:2134–2146.
46. **Suzuki, T., K. Ishii, H. Aizaki, and T. Wakita.** 2007. Hepatitis C viral life cycle. Adv. Drug Deliv. Rev. **59**:1200–1212.
47. **Tani, H., Y. Komoda, E. Matsuo, K. Suzuki, I. Hamamoto, T. Yamashita, K. Moriishi, K. Fujiyama, T. Kanto, N. Hayashi, A. Owsianka, A. H. Patel, M. A. Whitt, and Y. Matsuura.** 2007. Replication-competent recombinant vesicular stomatitis virus encoding hepatitis C virus envelope proteins. J. Virol. **81**:8601–8612.
48. **Timpe, J. M., Z. Stamataki, A. Jennings, K. Hu, M. J. Farquhar, H. J. Harris, A. Schwarz, I. Desombere, G. L. Roels, P. Balfe, and J. A. McKeating.** 2008. Hepatitis C virus cell-cell transmission in hepatoma cells in the presence of neutralizing antibodies. Hepatology **47**:17–24.
49. **Wakita, T., T. Pietschmann, T. Kato, T. Date, M. Miyamoto, Z. Zhao, K. Murthy, A. Habermann, H. G. Krausslich, M. Mizokami, R. Bartenschlager, and T. J. Liang.** 2005. Production of infectious hepatitis C virus in tissue culture from a cloned viral genome. Nat. Med. **11**:791–796.
50. **Witteveldt, J., M. J. Evans, J. Bitzegeio, G. Koutsoudakis, A. M. Owsianka, A. G. Angus, Z. Y. Keck, S. K. Foung, T. Pietschmann, C. M. Rice, and A. H. Patel.** 2009. CD81 is dispensable for hepatitis C virus cell-to-cell transmission in hepatoma cells. J. Gen. Virol. **90**:48–58.
51. **Yagnik, A. T., A. Lahm, A. Meola, R. M. Roccasecca, B. B. Ercole, A. Nicosia, and A. Tramontano.** 2000. A model for the hepatitis C virus envelope glycoprotein E2. Proteins **40**:355–366.
52. **Yi, M., Y. Ma, J. Yates, and S. M. Lemon.** 2009. Trans-complementation of an NS2 defect in a late step in hepatitis C virus (HCV) particle assembly and maturation. PLoS Pathog. **5**:e1000403.
53. **Zhong, J., P. Gastaminza, G. Cheng, S. Kapadia, T. Kato, D. R. Burton, S. F. Wieland, S. L. Uprichard, T. Wakita, and F. V. Chisari.** 2005. Robust hepatitis C virus infection in vitro. Proc. Natl. Acad. Sci. U. S. A. **102**:9294–9299.
54. **Zhong, J., P. Gastaminza, J. Chung, Z. Stamataki, M. Isogawa, G. Cheng, J. A. McKeating, and F. V. Chisari.** 2006. Persistent hepatitis C virus infection in vitro: coevolution of virus and host. J. Virol. **80**:11082–11093.

B型肝炎ウイルス感染の病態と治療法 5
免疫療法：過去からの教訓と未来への挑戦

Akbar Sheikh Mohammad Fazle

アクバル シェイク モハマド ファズレ：東芝病院 研究部

● はじめに

B型肝炎ウイルス（HBV）に起因する肝障害は，主に宿主の免疫応答により惹起される。先人たちの努力により積み上げられたエビデンスによれば，HBVの排除や持続感染のみならず，B型慢性肝炎（CHB）の病態にも，HBV-specificな免疫応答が深く関与している[1]。

CHBの今日的治療は，ラミブジンやエンテカビルなどの核酸アナログ製剤や，インターフェロン（IFN）などを用いた抗ウイルス療法が主流である。核酸アナログはHBVの複製を阻害し，強力な抗ウイルス作用を示す。そのため，血中のHBV-DNAの消失率が高い。しかし，核酸アナログでcccDNAまでをも消すことはできない。さらには，核酸アナログは免疫賦活作用をもたないため，HBe抗原，HBs抗原の消失とHBe抗体，HBs抗体の出現（セロコンバージョン）率が低い。また核酸アナログには，中止のタイミング，耐性株やbreakthrough hepatitisなどの問題点もある[2]。一方IFNは，抗ウイルス作用は核酸アナログほど強力ではないが，免疫賦活作用を備えているため，核酸アナログより高率のセロコンバージョン率を示す。しかしながら，IFNにはさまざまな副作用があるうえ，抗ウイルス効果も十分とはいえない[3]。興味深いことに，1989～2008年に行われたCHBに対するすべての無作為化比較対照試験のメタ解析によると，いずれの抗ウイルス療法も種々のパラメータを一時的に改善するものの，最終的な転帰と合併症については改善しなかったとされる[4]。

わが国にはHBVキャリアーが約100万人，世界には数億人存在すると推定されており，副作用が少なく，より効果的な（願わくば安価な）治療法が待望されている。そこで，CHBの病態の根本に存在する“HBV-specific immune response”に着目した免疫療法は，既存の治療法にとって代わる新しい（かつ安価な）治療法として期待されている。HBVの治療法確立の遅れの一因には，HBV感染モデル系の欠如あるいは不足をあげることができる。HBVに対しナチュラルな感染感受性を示す動物はチンパンジーなどの高等霊長類に限られており，もしマウスを実験に用いようと思えば，遺伝子改変マウスやヒト肝キメラマウスなどの不自然な感染モデル系を作製せねばならない。それらのモデル系を用いて興味深い結果が多数報告されているが，それらの実験系は，ヒト生体内におけるHBVの感染，複製，排除を忠実に再現しているとは言い難い。よって，CHBの新しい治療法を確立するには，ヒトでの臨床試験が不可避であり，かつきわめて重要である。

本稿では，CHBに対する免疫療法の従来の概念，CHBの病態のエビデンスに基づいた新しい